Master's in Chemical Engineering

Investigations on the influence of particle size of wood pellets on plasma-assisted ignition

Master dissertation

of

Pedro Afonso Kasmirski de Moura

Developed within the course of dissertation

held in

IFK - Institute of Combustion and Power Plant Technology / University of Stuttgart

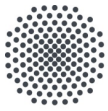

University of Stuttgart
Institute of Combustion and
Power Plant Technology

Supervisor at FEUP: **Prof. João Bernardo Lares Moreira de Campos**

Supervisor at University of Stuttgart: **M.Sc. Reyhane Youssefi**

U.PORTO
FEUP FACULDADE DE ENGENHARIA
UNIVERSIDADE DO PORTO

DEPARTAMENTO DE
ENGENHARIA QUÍMICA

March 2020

Acknowledgment

I would like to express my profound gratitude to the director of the Institute of Combustion and Power Plant Technology (IFK) Prof. Dr. techn. G. Scheffknecht for providing the opportunity to conduct this study. I also would like to acknowledge my supervisor at University of Stuttgart, M.Sc. Reyhane Youssefi for her guidance and support throughout my study, and to my supervisor at University of Porto, Prof. João Bernardo Lares Moreira de Campos for his assistance during this period. A special mention to each researcher whose work I have cited during the study.

Abstract

To enhance flexibility of conventional fossil fuel plants, a plasma-assisted ignition system is tested to be a substitute of existing start-up methods using oil and natural gas. Due to the high volatile content, biomass is studied as the start-up fuel for future power plants reduce CO_2 emissions and operation cost. Experimental investigations on the influence of biomass particle size on Plasma-assisted ignition are required to define the boundary conditions of the system. The large particle size distribution of the pulverized biomass contributes to difficulties on achieving ignition and stable flame formation.

On the experimental study, pulverized biomass is sieved into different particle shares and several fuel samples are produced. In a Pilot-scale 500-kW combustion facility with a swirl burner, the ignition behavior of each sample is evaluated at several different operational conditions, as result the critical share of the fine particles to reach successful operation is defined. Particle sizes bellow 100 μm were proven to be mainly responsible for the first ignition, fuel samples with possess less than 8.83 % of the critical share weren't able to achieve stable ignition at any operation condition. A technical economic study also evaluates the real possibility of installing the plasma ignition in an existing plant, the project proves to be economically viable with payback periods of 5.2 and 6.2 years for the two scenarios proposed in the study.

Keywords: Plasma-assisted ignition, pulverized biomass, techno-economic assessment.

Kurzfassung

Um die Flexibilität herkömmlicher Anlagen für fossile Brennstoffe zu verbessern, wird ein plasmaunterstütztes Zündsystem getestet, dass die bestehenden Anlaufmethoden unter Verwendung von Öl und Erdgas ersetzt. Aufgrund des hohen Gehalts an flüchtigen Bestandteilen wird Biomasse als Startbrennstoff für zukünftige Kraftwerke untersucht, um den CO2-Ausstoß und die Betriebskosten zu senken. Experimentelle Untersuchungen zum Einfluss der Partikelgröße von Biomasse auf die plasmaunterstützte Zündung sind erforderlich, um die Randbedingungen des Systems zu definieren. Die große Partikelgrößenverteilung der pulverisierten Biomasse trägt zu Schwierigkeiten beim Erreichen der Zündung und der stabilen Flammenbildung bei.

In der experimentellen Studie wird pulverisierte Biomasse in verschiedene Partikelanteile gesiebt und mehrere Brennstoffproben hergestellt. In einer 500-kW-Verbrennungsanlage im Pilotmaßstab mit einem Wirbelbrenner wird das Zündverhalten jeder Probe unter verschiedenen Betriebsbedingungen bewertet, wodurch der kritische Anteil der feinen Partikel für einen erfolgreichen Betrieb definiert wird. Es wurde nachgewiesen, dass Partikelgrößen unter 100 µm hauptsächlich für die erste Zündung verantwortlich sind. Kraftstoffproben mit einem Anteil von weniger als 8,83% des kritischen Anteils konnten unter keinen Betriebsbedingungen eine stabile Zündung erreichen. In einer technischen Wirtschaftsstudie wird auch die tatsächliche Möglichkeit der Installation der Plasmazündung in einer bestehenden Anlage bewertet. Das Projekt erweist sich mit Amortisationszeiten von 5.2 und 6.2 Jahren für die beiden in der Studie vorgeschlagenen Szenarien als wirtschaftlich profitabel.

Resumo

Para aumentar a flexibilidade das usinas tradicionais de combustível fóssil, um sistema de ignição assistido por plasma é testado para substituir os métodos de *startup* existentes que utilizam óleo e gás natural. Devido ao alto conteúdo volátil, a biomassa é estudada como combustível de *startup* para as usinas de energia, reduzindo as emissões de CO_2 e os custos operacionais. Investigações experimentais sobre a influência do tamanho das partículas de biomassa na ignição assistida por plasma são necessárias para definir as condições de operação do sistema. A distribuição de tamanho de partícula da biomassa pulverizada dificulta com que o combustível inicie ignição e formação estável da chama.

No estudo experimental, a biomassa pulverizada é peneirada em diferentes tamanhos de partículas e várias amostras de combustível são produzidas. Instalação piloto de combustão de 500 kW com um queimador de turbilhão, o comportamento de ignição de cada amostra é avaliado em diferentes condições operacionais, como resultado, é definido uma quantidade crítica que as partículas finas necessitam possuir para alcançar uma ignição bem-sucedida. Comprovou-se que os tamanhos de partícula abaixo de 100 μm são os principais responsáveis pela primeira ignição, as amostras de combustível com menos de 8.83% da parcela crítica não foram capazes de alcançar uma ignição estável em qualquer condição de operação. Um estudo técnico econômico avalia também a possibilidade real de instalar a ignição de plasma, o projeto se mostra economicamente viável com períodos de retorno de 5.2 e 6.2 anos para os dois cenários propostos no estudo.

Declaration

I hereby declare, under word of honor, that this work is original and that all non-original contributions are indicated, and due reference is given to the author and source

16/03/2020

Sign and date

Index

List of Figures

List of Tables

Notation and Glossary

$\dot{V}$	Volumetric Flow	$m^3{}_N \cdot h^{-1}$
Δ	Variation	
c	Concentration	
d	Diameter of plasma nozzle	mm
$\dot{M}$	Mass Flow	$kg \cdot h^{-1}$
$O_{min,dry}$	Minimum Oxygen demand, dry	$m^3{}_{N,O_2} \cdot h^{-1}$

List of Indices

t	Time
TA	Total air flow
f	Fuel

List of Acronyms

IFK	Institute of Combustion and Power Plant Technology
KSVA	Kohlenstaubverbrennungsanlage
PF	Power Factor
ASTM	American Society for Testing and Materials
DIN	Deutsches Institut für Normung
ISO	International Organization for Standardization
a.r	As Received
w.f.	Water Free

1 Introduction

The energy transition from fossil fuels to renewable energy sources necessitates flexible operational regimes for conventional fossil fuel plants. To increase the flexibility, an advanced start-up system has been developed, a plasma-assisted solid fuel ignition systems, which can be a substitute for existing start-up methods using oil and gas. The utilization of biomass within this system offers a new prospect for future biomass plants to operate with zero to negative CO_2 emissions.

1.1 Problem definition

To use woody biomass as the start-up fuel within the plasma ignition systems, experimental investigations are required to define the boundary conditions of the system. To obtain an optimized plasma ignition system, the required chemical and physical properties of the fuel needs to be determined. Woody biomass with high volatile content represents significant potentials to be used for the plasma ignition system. However, due to relatively large particle sizes of the pulverized biomass, difficulties are expected to achieve ignition and stable flame formation.

1.2 IFK – Institute of Combustion and Power Plant Technology

IFK was built on 1958, together with the power plant, due to supply needs of the university campus, the institute deals with thermal power plant technology and power grid systems. The IFK possesses several lab-scale research facilities, and experimental test rigs making the institute unique in Germany.

1.3 Objectives

Investigations are required to define the influence of particle size on the ignition and to determine the critical share of the fine particles to reach successful operation. Pilot-scale experiments will be performed at the 500 kW combustion facility using woody biomass with different particle sizes. Besides the experimental activities, a techno-economic study will be performed on the plasma ignition system to be retrofitted in existing power plants.

1.4 Task description

1. Literature review on plasma ignition system and biomass ignition;
2. Performing a techno-economic study for plasma ignition system;
3. Fuel preparation (milling and producing different particle size distribution);
4. Execution of ignition tests in the 500-kW facility;
5. Evaluation and interpretation of the experimental results;

2 Literature Review

In the following section the state of the art is discussed on the current situation of renewable energy and biomass as fuel; afterward, relevant literature on biomass ignition and combustion processes are discussed, with special detail to relevant details on the effects of particle size. Following, a brief overview in pulverized fuel systems and current studies start-up methods, with focus on plasma ignition. Finally, a techno-economic assessment focusing on the benefits of retrofitting the plasma ignition system on existing power plants is presented.

2.1 Present situation

Increasing the share of renewables in the primary energy market is important in order to deal with the world climate change. As new environmental protection policies are put into action, the share of clean energy is steadily increasing within the power industry, powerplants face the challenge of load flexibility. Many units were designed to work as base load plants, and now need to work as puffer-load units. These power plants units face more start-ups, stops, and smaller load operations. Renewables are manly comprised of volatile energy generation (e.g. Wind power and Solar Power), which are not able to maintain a stable production, this makes it necessary to compensate sudden fluctuations with solutions that allows load and operation flexibility in a competitive price [1].

During many years, conventional fossil fuel plants were designed and operated with coal as main fuel. Working at a constant rated efficient, coal is considered to be a cheap fuel, with great availability worldwide, easily mined from nearby locations and offers steady combustion characteristics. The impact of using such fossil fuels nowadays, make us realize the importance to seek different possibilities to generate energy but with a smaller footprint on the environment. This brings the necessity to use solutions with zero carbon footprint on the environment, many countries have new regulations seeking to reduce the greenhouse effect, and several of those countries are committed to achieve the desired levels even in the short run, these new regulations are created with the goal to enforce liability within the environment. Germany's government energy concept aims to reduce the greenhouse gasses emissions of energy generation plants by 2050 to 80-95% over the levels in 1990. With different strategies, the government seeks to provide reliable and affordable energy while maintaining the environmental protection [2]. According to Scheftelowitz et al. (2018), by the end of 2015, approximately 31.6% of the German gross electricity consumption was provided from renewable energies, 7% being from biomass. Coal still accounted for 45% of the generated electricity supply in Germany on the same year [3]. The coal phase-out is indispensable not only to reduce

greenhouse gasses emissions, but to also meet the desired limit thresholds to continue operation [4].

Operation with the minimum technical load also brings challenges to the plant, as changes with different quality of fuels can affect the combustion, ignition systems are required to guarantee stable combustion in different load conditions. Oil is traditionally used worldwide as auxiliary fuel and provides the start-up and stabilization of the plant. While expensive, oil is also very polluting, producing a tremendous amount of hazardous emissions [5]. High reliable and economic ignition methods are necessary as the cost associated with each start-up needs to be reduced. To avoid shutdown due to costs and emissions policies, power plants have to retrofit its auxiliary oil ignition system by new methods of ignition that allows an oil-free operation.

2.2 Biomass

Biomass is an important renewable fuel, its use to the production of electricity has grown in the more than ever. As mentioned, the worldwide increased awareness concerning the limited availability of fossil fuels, and creation of more strict environmental policies and regulations that seek to diminish the current dependence on fossil fuels, has arouse a global interest in alternative fuels [6]–[8].

2.2.1 Definition

Biomass is any biodegradable and non-fossilized organic material used as source of fuel, and it's manly composed of three components: lignin, cellulose and hemicellulose. There are a wide range of biomass fuels available in the environment, and they are classified on their origin and properties. Divided into four types such as primary residues, secondary residues, tertiary residues and energy crops. Primary residues are generally obtained from the by-products of forest and food crops, and include biomass such as wood, straw, cereals, maize, etc. Secondary residues include saw and paper mills, normally derived from processing biomass material for industrial use. Tertiary residues are derived from other used materials, and include waste and demolition wood, etc. Energy crops is the type of biomass grown only for energy production, and later burned to produce heat and energy [9], [10].

Biomass characteristics vary greatly, not only in size and shape, but some can be wet, causing to become sticky, many also tend to be compressible and pliable. Some materials are fragile where they can be easily fractured, whereas others may be stringy and resilient [11].

2.2.2 Benefits and environmental status

Biomass being renewable and CO_2-neutral, its use offers the advantage of maintaining the carbon cycle, as during it's growing cycle, biomass absorbs CO_2 form the atmosphere, while the

same amount is released during the combustion. Biomass is considered to be a promising source of renewable energy for mitigating climate change [6]–[8], [12].

Thru photosynthesis, biomass is able to store solar energy as chemical energy during grown of plants and trees, energy which is released when combusted. Although biomass is a CO_2 neutral energy resource, its usage as fuel is in the early stage of applications was discouraged during a long time due to its corrosive and slagging issues. 62 countries publicly produce energy using biomass as fuel [9], [10].

As quality variates, its moisture content also varies, biomass is often known to contain considerable amount of water, and the high moisture content will affect negatively the performance of the biomass combustion, pre-treatment is commonly done to reduce water content before combustion it. The melting point of dissolved ash can be lower when compared to other fuels and may cause slagging and fouling problems. This requires not only a great availability of grade biomass to be used, but also better and more efficient conversion processes for energy generation. Certified quality biomass ensures low ash, Sulphur and moisture content. But large scale power plants may need flexibility with the fuel when comes to quality to reduce operation costs [6], [8], [9], [13], [14].

Fatehi, Schmidt, & Bai, (2018) pointed in studies that biomass has great potential in generating heat and power via thermochemical conversion. But there are still challenges within its combustion, as efficiency, pollutant emissions, ash deposition, corrosion and fuel flexibility still need to be addressed for a safe fuel switch. Correctly understanding the processes occurring during the combustion is mandatory for a proper optimization of its combustion processes. Biomass is known to have a low ignition and burnout temperature, as well as a high combustion rate, due to a higher volatile and low ash content [16], [17].

2.3 Biomass Ignition and Combustion

The ignition and combustion of biomass is a process that will depends both on fuel properties and combustion application. It can be divided into three main stages: Drying, release and ignition of volatiles, combustion of fixed carbon [18]. Figure 2.1 illustrates the main steps in the combustion process.

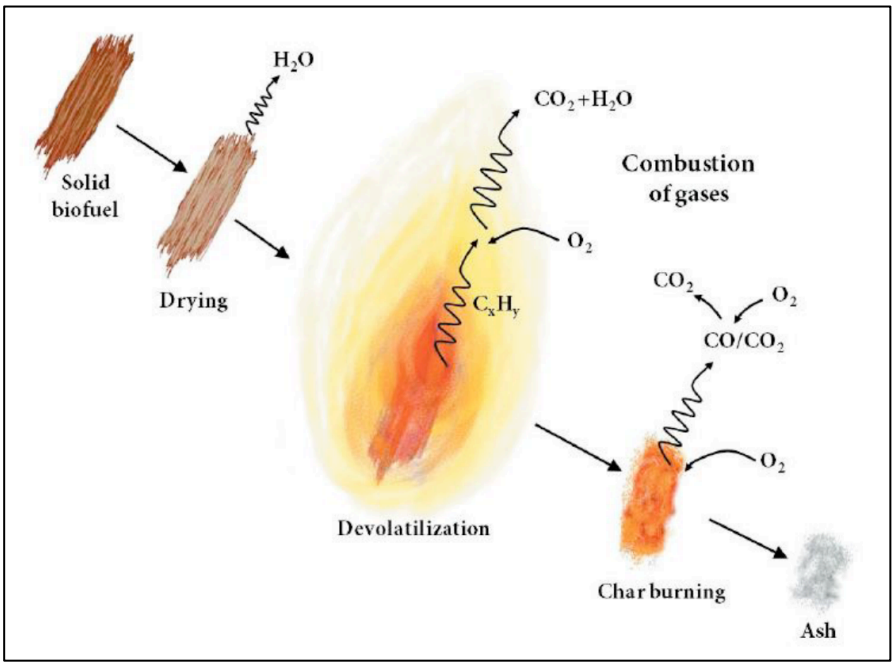

Figure 2.1 - Schematic of solid biofuel combustion process [18]

Even though co-combusted with other fuels in similar conditions, biomass properties are different when compared to another fuel as coal. Biomass offers faster reaction rates, non-uniform gas evolution profile, and longer volatile combustion duration. However, these behaviors can differ widely with different types of biomass, different physical structures and chemical compositions influence the operating efficiency, making a more demanding task to evaluate and define the best operating conditions [19]. As coal has a higher energy density, Biomass particles require a larger particle sizes to achieve similar thermal throughput. Highly volatile materials, lower carbon content, lower heating value, and high moisture content are some differences in its characteristics. Determining the quality is an important parameter which will define its acceptance as fuel to be combusted [19]–[21].

Due to the challenges encountered with the combustion of biomass that are not normally seen with coal, most recent studies on solid fuel combustion derive from previous coal studies, and of the idea to switch from coal to biomass, but even so, there is a lack of knowledge and information in the use of biomass as fuel [18].

When comes to ignition, the high moisture content brings a challenge when igniting the particle and may lead to problems with flame stability. Important parameters as distribution of temperature and conversion rate of biomass are strongly affected by the process occurring in the particle. The ignition process of a biomass particle is normally dominated by the volatile combustion. Once ignited, the biomass burning rate normally increases, which is attributed to the rapid release of volatiles and the high porosity of the char particles [22]. The conversion of a biomass particle is normally divided between processes that occur inside the solid structure of the particle and processes that occurs outside, in the particle boundary layer [15]. Important

differences between the ignition delay time, volatiles combustion time and soot formation propensity of the biomass residues, which are mainly affected by the biomass volatile matter content. For small pulverized fuel particles, the temperature across the particle is assumed to be constant during drying and devolatilization steps [23], [24].

Wang et al., (2012) studied the co-firing of biomass in a pulverized coal fired boiler, in its findings, biomass was easily ignited and burned out, mainly to the higher volatile content and lower ash content. Three noticeable regions were detected for all samples: water evaporation, volatile combustion and fixed carbon burning. Mean ignition, burnout and the peak temperatures of cornstalk increased with the elevation of heating rate, which is noted to be a disadvantage in biomass combustion, but the reaction rate increased at higher heating rate.

Ballester, Barroso, Cerecedo, & Ichaso, (2005) studied the behavior of three pulverized fuels in a semi-industrial furnace, bituminous coal, lignite, and biomass. In their findings, the operation conditions of the biomass were similar to the coal, but as expected, the higher volatile content of the biomass leaded to intensive flames close to the burner. The Authors suggested that two different regions can be noticed in the biomass flame: the first is a zone of intense combustion close to the burner, and a second zone, where the larger biomass particles gradually devolatilize and are consumed.

2.3.1 Drying

The first stage corresponds to the water evaporation step. The process begins when moisture changes into gaseous phase and moves through from the inner pores to the surface. The process is endothermic and controlled by the transfer of mass and heat. Once exposed in the high temperature furnace, the biomass particle is heated up by the surrounding furnace wall and oxidizing agent via radiation and convection, resulting in a rise in the surface temperature of the biomass particle. A thin moisture-evaporation front in the particle surface is stablished [24], [26]. The drying occurs from the surface and the pores, as ignition energy is supplied to the particle.

As the moisture evaporation progress is limited by the transport of heat inside the particle, the drying stage rate is not constant, as the particles will not be able to provide a constant supply of moisture during the whole drying stage. A rising rate period is seen due to the increasing temperature in the particle, as free water will escape in the form of vapor. When there is insufficient free moisture, the drying rate starts to decrease and becomes to be controlled by the moisture diffusion from inside the particle to the surface, until the particle is dried and the rate reaches zero [14].

In the literature is possible to come across different kinetics models for the biomass drying step that can help understand the different behaviors of this stage, Fick's second law is commonly

used to explain the drying process of most biological materials. If moisture content is too high, pre-drying of the fuel may be employed, doing so, increases fuel quality prior to combustion [8], [14], [27]–[30].

2.3.2 Devolatilization and Ignition

The second stage describes the devolatilization and subsequent ignition of volatile gases. During this stage, the devolatilization step is preeminent as biomass possess a high volatile content, and most of available energy contained in the particle is released. High furnace temperatures promote the devolatilization step, which is highly sensitive to the particle temperature. The drying and devolatilization rates will increase when particle temperature increases. The released amount of volatile matter is mainly dependent on fuel characteristics and devolatilization conditions, as the heating rate and temperature of the furnace [26].

There is a common assumption that the rate of devolatilization is represented by a first order Arrhenius equation. The main believe is that pulverized fuel particles are thermally thin, so the reaction temperatures are uniform throughout the particle, and that there is no secondary reaction leading to the deposition of cracked products [24]. Rezaei, Sokhansanj, Bi, Lim, & Lau, (2017) found during their work that particles smaller than 500 μm are free of any internal heat transfer limitation.

Shortly after, the devolatilization process begins, the released volatile gases ignite and a flame envelope surrounding the particle is formed [24]. The ignition process is initiated by oxidation reactions on the particle surface, and then the volatiles form a homogeneous diffusion flame away from the particle surface. A strong heat release and rapid increase in temperature originates a self-sustaining combustion process.

It may occur three different types of ignition behaviors, homogeneous, heterogeneous, or a combination of both. Homogeneous ignition is given when first ignition happens in the gas phase (before ignition of the solid residue), this forms a flame envelop around the particle, and doesn't allow oxygen to reach the particle surface. Heterogeneous ignition normally occurs at high heating rates, if the particle surface reaches ignition temperature before sufficient volatile release, a direct oxygen attack can react with the char, igniting the solid surface before the volatiles. A hetero-homogeneous ignition happens if the first ignition in the gas phase occurs close to the surface and will not be able to form a flame envelop around the particle [32].

With the increase of the furnace temperature, ignition time will decrease as the amount of released volatiles increases. The species, rate and amount of released volatiles during ignition and combustion process are highly dependent of fuel type and its heating condition. At sufficiently high temperature, the biomass particle could ignite before the start of

devolatilization, indicating that a heterogenous ignition has occurred at the particle surface [28].

Biomass ignition behavior can be controlled by adjusting the degree of devolatilization, particle size and surrounding gas temperature. Thru that, pulverized biomass combustion process can be optimized [28]. An increase in the oxygen concentration is known to intensify the local heat release as its speed up the homogeneous combustion of the released volatiles [17].

Effect of Particle Size and Shape

The particle size of the solid fuels has an important impact on their combustion, in bigger particles, drying and devolatilization may occur simultaneously until the biomass particle is completely dried. Particle size is an important characteristic parameter that will define the ignition mode [33]**.** Finer particles will be ignited immediately, and the majority of its heat is released rapidly. Increasing the particles size will increase the minimum required ignition temperature, as well as the particle residence time in the furnace, as larger particles required higher temperatures to ignite [28].

Even though particle devolatilization is well defined in the literature, it's important to notice that studies, which illustrate the different effects of biomass particle size and shape on ignition and devolatilization for pulverized biomass is scarce.

Weng, Costa, Aldén, & Li, 2019 studied particle ignition and combustion of four different pulverized biomass particles in the range of 224-250 μm. The Authors evidenced merely small differences in the biomass combustion behavior, these differences were assumed to be based on the origin, type and pre-treatment of the biomass. It was concluded that ignition of the biomass particles normally occurred in the gas-phase, and that there was a decrease in the ignition delay time as the mean gas temperature increased. The four different biomass char particles presented heterogeneous oxidation after the extinction of the homogeneous combustion of volatiles.

The study of Steer et al. (2015) focused on the effects of particle grinding on the burnout and surface chemistry during coal combustion suggested that the process of grinding alters the physical properties of the samples, so that in some cases the larger size classification gives improved combustion burnout profiles when compared with smaller sizes.

Lu et al., (2010) studied the effects of different biomass particle sizes and shapes on devolatilization. The assumption of spherical particles is a misconception, as in practice the biomass particles are not able to be milled into spherical particles as coal. The Author distinguished the particles into sample groups, near-spherical, flake-like and cylinder-like, all three samples had similar volumes and mass, but different areas and shapes. Model predictions and experimental data showed a slower mass loss from the near-spherical particles when

compared to the others, while the flake-like particles are devolatilized faster. Effects of particle shape on conversion time is less relevant in smaller particles, as larger particles will present internal temperature and heat transfer gradients.

Tar is a major product of the devolatilization process. It has been reported by Yang et al., 2008, cracking of tar may occur inside the particle, and it's an issue to determine whether the tar evaporates or remains as a carbonaceous product in the biomass particle. Wood has a forcible ability to crack the tar into lighter molecules at elevated temperatures.

2.3.3 Combustion

The third stage corresponds to the combustion step. As mentioned previously, there are two types of different combustion happening, combustion of volatiles and combustion of char, which happens first will depend on the ignition step. Biomass is tendentious to first a combustion of volatiles, then char combustion due to the high particle volatile content as already mentioned.

Combustion of volatiles is fast but with a smooth progressive flame growth. Due to high porosity of biomass particles, the volatile matter flows through the porous to the vicinity of the particle and are combusted [13]. As mentioned in the previous subsection, the homogeneous combustion of the volatiles performs a very important role in whole combustion process. Ignition, local stoichiometries, flame stability and pollutant emissions will be directly dependent of the volatiles combustion [33].

Once the volatiles are combusted, combustion of char proceeds, the particle volume shrinks, char will start to burn only when the devolatilization approaches the final stage. A circular char-burnout front will be formed, which travels inward and leaves an ash "shell" behind. Char-burning process may overlap with the devolatilization process, if particle size is big enough, but normally is not seen in pulverized fuel combustion [24].

The char combustion mechanism can be considered complicated, as it affected not only by the biomass composition but also by the non-spherical geometry of the fuel particles. Biomass char more reactive than coal char, and its combustion has been outlined by some authors, but there are uncertainties of the reaction order with respect to the oxygen concentration, normally is accepted a reaction order of one, which has been used by some authors [24], [36]. During combustion, no diffusion resistance due to ash is assumed, since the ash content of biomass is low and the ash is fragile [37].

During combustion, small particles can leave the burner without being combusted. These particles have such small size that their capture by the gas treatment system is inefficient. With that, there is a possibility of high Particulate Matter (PM) emission and this represents an important issue to the human health and to the environment around [19].

Ordinary biomass is known to contain in its composition a set of diverse elements, Al, Ca, Fe, Mg, P, S and Si, are the mostly commonly found. Many of these elements actively participate in reactions that induce ash fouling and slagging problems in combustion systems. Potassium is reported to be the most critical, it offers a direct influence in the ash behavior, and in the corrosion chemistry. An important plant nutrient, potassium is found in high concentrations in many types of biomass fuels, is highly mobile, and it is absorbed into woody material through the root system and transported to all areas of the growing tree [38]. It has a catalytic behavior at high heating rates and temperature conditions, which influence both devolatilization and char burn-out stages. In the presence of potassium, the particle retains its structural integrity until the end of carbon burn-out when it starts to collapse and shrink. In the absence, the particles melt, and combustion resembles that of an oil droplet combustion, and the char residue is burned-out at an extremely slow rate [38].

Evaporation of metals during biomass combustion is also reported to occur under certain circumstances. Yang et al., (2008) studied the biomass particle metal release mechanism, during the devolatilization and char burning step. And their findings were that metal release can be catalyzed in the presence of potassium.

2.4 Pulverized Fuel Systems

Pulverized fuel systems are normally employed in an industrial or utility boiler that generates thermal energy by burning pulverized fuel that is blown into the furnace. The main idea of a pulverized fuel firing system is that if that if the fuel particles are fine enough, the combustion will happen practically as simply and efficiently as gas fuel [39]. Pulverized fuel systems have been used for almost a century, generating combined power and heat in utility boilers. Within the years, developments and scientific studies allowed increase in efficiency, allowing the use of such boilers as primary energy resource for many years [40].

2.4.1 Pulverized Biomass

As was already discussed in the previous section, the combustion properties of biomass are naturally different to those expected from coal, the challenges in existing pulverized coal boilers when switching to biomass is keeping the same output, while maintaining high efficiency and a stable operation [26]. Pulverized biomass fuels can be burned in a flame the same way as other fuels, particles are reduced to an adequate size range that can guarantee a complete burnout during the short period of time inside the burner. Delayed combustion may cause the combustion zone of the biomass to extend towards the furnace exit, causing an unexpected overheating of the super-heaters.

Specific particle properties as size, shape and density, play main role on particle flow and flame propagation in pulverized fuel combustion. Efficient milling of biomass to an acceptable size

distribution is considered one of the main bottlenecks in the combustion on systems where particle sizes need to be <1000 μm. The milling process is energy demanding and result in fibrous materials with low bulk densities, which has been reported to be associated with particle transport problems [11], [41].

As mentioned in previous section, during pulverized combustion the size of a biomass particle in is expected to be larger than that of a coal particle due to lower particle density and faster devolatilization rates. As the reactivity of biomass is higher than coal, sieving the biomass as fine as coal won't be necessary, biomass particles burn out quickly, even at bigger sizes. Due to different milling behavior and for economic reasons, pulverizing biomass to the same size as coal particles is expensive and discouraged [17], [20], [28].

Biomass particle size will influence on ignition delay, thus is essential to determine the preferable size of its particles. Much is discussed but is still unclear the effects of particle size on the ignition delay and combustion process [28], [30]. Jiménez et al., (2008) realized experiments to determine the kinetics of devolatilization and oxidation of pulverized biomass. The fuel was grinded and respectively sieved in the range of 300-400 μm. The range was decided considering the respective quality of biomass. The presence of soil particles in the sample which was mainly found in the < 300 μm particle size class is prone to influence in the analysis, so selecting the particle size may reduce the impact of the extraneous material. The most common size range of pulverized biomass systems is of 10-1000 μm [6], [24], [26].

When milling biomass, the pulverized wood may have either a spherical or a cylindrical structure, where straws only have a cylindrical structure. Spherical particles have the longest conversion time for the reason that they have the lowermost possible surface area/volume ratio. Non-spherical particles shapes support a fast and complete conversion. The aspect ratio is determined by the degree of milling [17], [24]. Momeni et al. (2013) in its studies, pointed out that, first pelletizing the raw biomass, then separately pulverizing the pellets in coal mills, is of great interest, as it allows the material to obtain smaller particles when compared to just normally pulverizing the biomass in the coal mills.

As it was already mentioned, the most relevant parameter that needs to be define is the particle size. How large could the particle be when firing pulverized biomass so is feasible to have a stable and efficient combustion. An increase in particle sizes, may decrease the particle burnout performance as higher amount of char are formed at lower heating-up rates, which is normally expected in large particles. Similar to what was reported in pulverized coal studies [33], [37].

When switching fuels, design and operation schemes have to be revised, adapted to those new fuels. Jiménez et al., (2008) addressed two main difficulties during a biomass fuel switch. The

high concentration of mineral matter in the biomass, may cause operational problems related to the low melting temperature of ash, corrosion enhancement, and the generation of fine particles. The design and adaptation of the rig to the new fuels, requires a good knowledge of the fuel reactivity. Even though coal combustion studies are well stablished, biomass brings certain uncertainties, with very scarce data available on the combustion behavior in pulverized fuel combustion.

In pulverized coal combustion, neglecting the temperature gradients inside the particles, and assuming that particles behave as thermally thin, has been the accepted in the past years, but with biomass, particles have irregular shapes, different lengths, and so on. The assumption of thermally thin particles may not be adequate for the upper size range employed on pulverized biomass combustion. Yang et al. (2008) ensures that a new approach has to be developed. Jiménez et al. (2008), acknowledged according to calculations that the thermally thin model may be employed to pulverized biomass particles sizes up to 500 μm. And practically half of the total burnout time is devoted to the release of the volatiles, a fraction much greater than the typical values for pulverized coal combustion, and directly attributable to the high volatile content of the biomass.

S. Li, Xu, Liu, Yang, & Lu, (2004) experimented single biomass particle combustion in a drop tube furnace. In their findings, the amount of char residue increased about 20%, when the particle size increased from 500–700 μm to 700–1000 μm. Saastamoinen et al. (2010) conducted a study of pulverized biomass particle burnout in large boilers. Particles under 500 μm were burnt in all studied scenarios and almost the case for particles of 1000 μm size. According to the authors calculations, a 500 μm biomass particle will have the same burnout time as a 200 μm Polish coal particle at 1373 K.

The milling process used to fractionate the particles, results in a wide distribution of size and shape parameters. Large biomass particles impose some limitations to the efficiency of the system. Turbulent flows with non-spherical particles of irregular shapes, the particle dispersion characteristics and velocity profiles can be significantly different than for spherical particles [43]. Particle size is expected to have noticeable effects on process characteristics. As already mentioned, there is a lack in studies of particle size effects on combustion behavior of pulverized biomass. Moreover, the very few studies available in the literature concentrated either in just one wide range or in just one narrow range of biomass particle sizes [33].

2.4.2 Startup Methods

In a conventional pulverized fuel combustion boiler, fuel is mixed with primary air, fed to the burner and combusted with secondary air in the furnace. Stable combustion is sustained if flame and radiation from the furnace wall give sufficient energy. During startup or overloading of the

burner, auxiliary energy is mandatory to heat the fuel particles and maintain sustainable combustion. Auxiliary methods, as burning oil, must be employed to support the combustion in the furnace [44]. Low temperature in the furnace during combustion makes an efficient self-sustaining combustion impossible. Plant operators are faced with the necessity to introduce additional thermal energy into the system in order to provide continuous stable combustion. Limiting factors in pulverized fuel systems are the particles heating rate and short residence time of the air–fuel dust mixture in the duct. Furnace heating is often realized by combustion of reserve or auxiliary fuel, normally oil, or natural gas, which are easily burned at ambient temperatures. The start-up process of a utility pulverized fuel fired boiler can last up to 2-3 hours [45].

Looking from the economic point of view, different technologies of boiler start-up that avoid the use of oil may be more cost effective. Due to elevated costs of oil, research and development of new technologies and methods of ignition are necessary to replace the use of liquid fuels. The switch to safer, less reactive and stable fuels also brings an increase in fire safety for the facility while reducing emission of harmful components into the environment [5].

Some methods for start-up of the burners are: Liquid auxiliary fuel burner (Figure 2.2), electric heater (Figure 2.3) or plasma torch (Figure 2.4) are some examples.

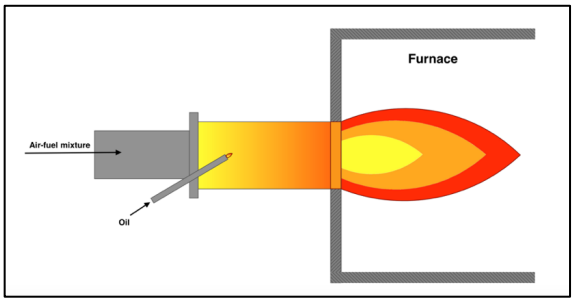

Figure 2.2 - Scheme of fire burner with auxiliary fuel

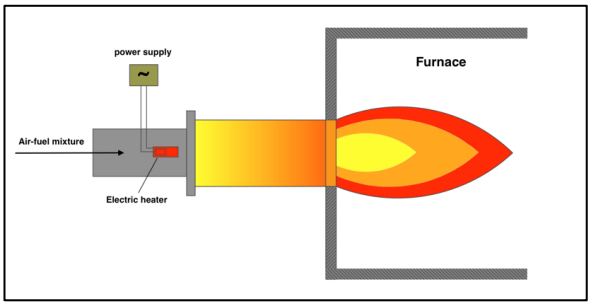

Figure 2.3 - Scheme of fire burner with electric heater

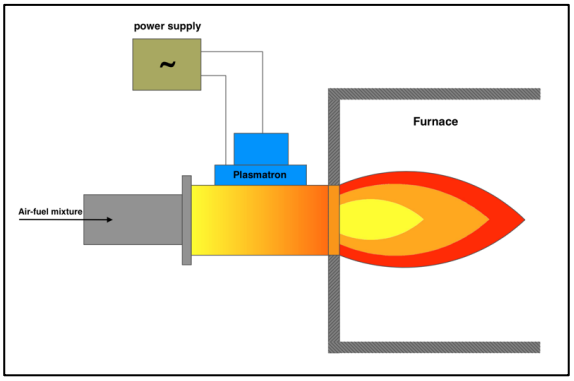

Figure 2.4 - Scheme of fire burner with plasma torch

The effectiveness of each type of burner can only be determined individually. Important parameters as the dimensional characteristics and operating modes (primarily temperatures) have to be defined to ensure stable ignition and combustion of the fuel dust/air mixture.

W. Li, Cen, Zheng, Zhou, & Cao, (2004) introduced the idea of an induction-heating ignition burner for the pulverized fuel stream. When turned-on, the induction system heats the metal alloy tube surrounding the fuel stream, an air-fuel mixture is ejected thru the tube and ignition occurs. Figure 2.5 shows a schematic diagram of the set-up. The induction-heating burner is said to be highly reliable and cost-effective in full-load and part-load operations.

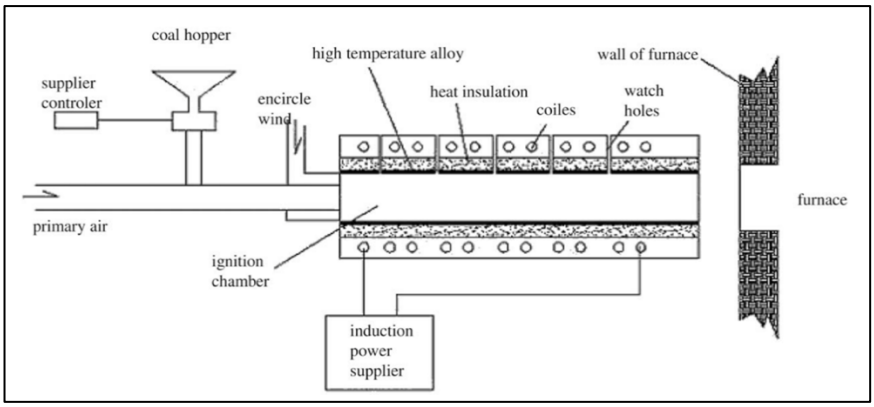

Figure 2.5 - Schematic diagram of induction-heating ignition burner [45].

2.4.3 Plasma Ignition Systems

As mentioned in the previous section, the purpose of any boiler start-up procedure is mainly to heat the furnace and achieve the minimum temperature necessary to initiate sustainable combustion of the primary fuel. Instead of usual and expensive systems of heavy oil or natural gas burners for fuel ignition, plasma torches are studied to replace old and expensive methods in order to achieve great savings during boiler start-up [46]. A Plasma Ignition system works by ionizing a gas medium to obtain a plasma with stable power and temperatures over 5000 K. The fuel is rapidly ignited, by creating a local high temperature section, the particles immediately release their volatiles and break-down [47].

After 20 years of development, plasma assisted ignition has made great advancement in its field [47], [48]. Plasma burners are able to offer stable combustion, with fast fire rates and controllable temperatures. Increased efficiency in fuel combustion, no use of auxiliary fuel, and reduction of harmful emissions, plasma ignition systems are believed to be ready to replace oil-fired start-up systems in pulverized fuel-fired power plants, improving operation conditions, while accomplishing an oil-free operation [47]. Figure 2.6 shows a sketch of a plasma assisted fuel combustion.

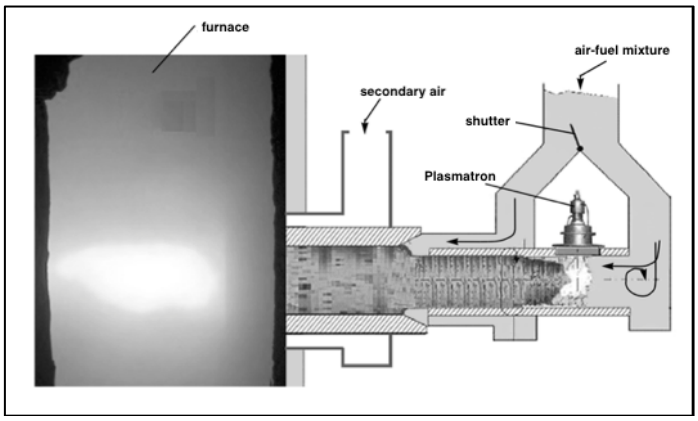

Figure 2.6 – Sketch of plasma fuel system [49]

During assisted plasma ignition, a flammable mixture of volatile, fine particles of biomass and oxidizer is formed, ignited in the burner and then completely combusted in the furnace chamber. This ensures high temperatures in the burner muffle that are sufficient to implement a self-sustaining combustion process of pulverized biomass. The boiler furnace will be heated by the energy released by the pulverized-biomass torch [5].

Many authors describe plasma as an important technology, playing a crucial role in energy-saving emission reductions and to the construction of greener power plants. In China, at least 52 coal-fired power plants have reported to completely cancel their fuel-oil start-up system [47], [50]. In Turkey, during commissioning of two 600 MW coal-fired burner units that started operation in 2016, the oil-free start-up operation allowed to save an enormous amount of oil, contributing to a great economic and environmental benefits as the burners don't utilize a fuel oil system for start-up [47].

2.5 Techno-economic assessment

The techno-economic assessment allows a more extensive cost evaluation of a given project, providing the perspective of the expected project payout. The main factor influencing costs when switching fuels, will be the change of associated operation costs, as fuel price, maintenance of specific facilities and taxes associated with emission of pollutants. It's also important to evaluate the impacts on pollution reduction, as it may be a reduction in compulsory taxes.

As mentioned before, pulverized fuel fired power stations have an expensive operation of its fuel oil systems, start-up operating costs can account for up to 10% of all operating costs [5]. The use of such system in a power plant, includes costs with fuel oil transportation, storage, conveyors, combustion devices and so on. Replacement of oil system with a plasma assisted ignition, allows the power plant to realize oil-free operation by burning uniquely a single fuel as biomass, bringing huge economic benefits along with enhanced operation safety. Plasma fuel systems eliminate the need of auxiliary fuels on start-up and stabilization of combustion [51].

Considering the investment and operation cost of firefighting, when realized single fuel operation, savings can be even greater as the fire pump can be simplified, and there is a reduction in danger by not burning the fuel oil [5].

According to Zhang et al., (2017), during the commissioning of a Turkish power plant, the initial investment on a plasma assisted ignition system was recovered even before the unit was put into commercial operation, as a large amount of oil is not burned, the costs associated with the auxiliary fuel oil are saved. The savings were estimated to be approximately 3 000 000 USD, which was more than 2 times of the investment cost associated with plasma ignition system for that facility.

2.6 Thesis Statement

Due to increasing environmental awareness, the change from fossil fuels to renewable energy production is crucial to reduce the carbon footprint. Hence, the objective of this study is to evaluate the ignition of different biomass particle sizes as a replacement for coal in a pulverized fuel burner integrated with plasma ignition system. Plasma systems has proven to provide more than enough energy to dry, devolatilize and ignite the fuel, and the literature shows that biomass possess the required characteristics to maintain steady combustion once ignited.

3 Experimental Facility and Methodology

The following chapter explains the experimental facility used to conduct the experiments in order to understand the combustion behavior of pulverized wood pellets on plasma-assisted ignition and determine the critical size distribution for a sustainable combustion. Detailed description of the pilot-scale facility is disclosed. Pertinent information of key components as description of the burner, plasma system, milling system and calibration of fuel feeder are listed below.

Physical and chemical analyses of the fuel and generated samples for this study are also reported. The parametric study layout used as standard test matrix for each sample run is presented and the methodology applied to evaluate the results is explained. As method of evaluation different shares of particles sizes was generated for this study, the procedure is explained below.

3.1 Description of the facility

The tests are performed at the Kohlenstaubverbrennungsanlage (KSVA) test facility, which is a 500-kW pilot-scale pulverized fuel combustion plant, available in IFK facilities. Designed to conduct research on solid fuel combustion, the rig consists of a four segments vertical down-fired combustion chamber. With inner diameter of 750 mm and the length of 7,000 mm, the first three segments of the combustion chamber include an extra refractory coating protecting the facility against extremely high temperatures. Only water cooling is employed in the rig, the water runs from the chamber bottom segment to the top segment, the fourth segment is also connected to an ash funnel, and generated ash can be collected at the bottom of the furnace. The flue gas cleaning system employs a $DeNO_x$ catalyst and an electrostatic precipitator installed in the flue gas channel, which can be separately by-passed. The test facility is equipped with a handful of measurement devices to investigate the several aspects of the pulverized fuel firing. Figure 3.1 is a sketch of the test facility.

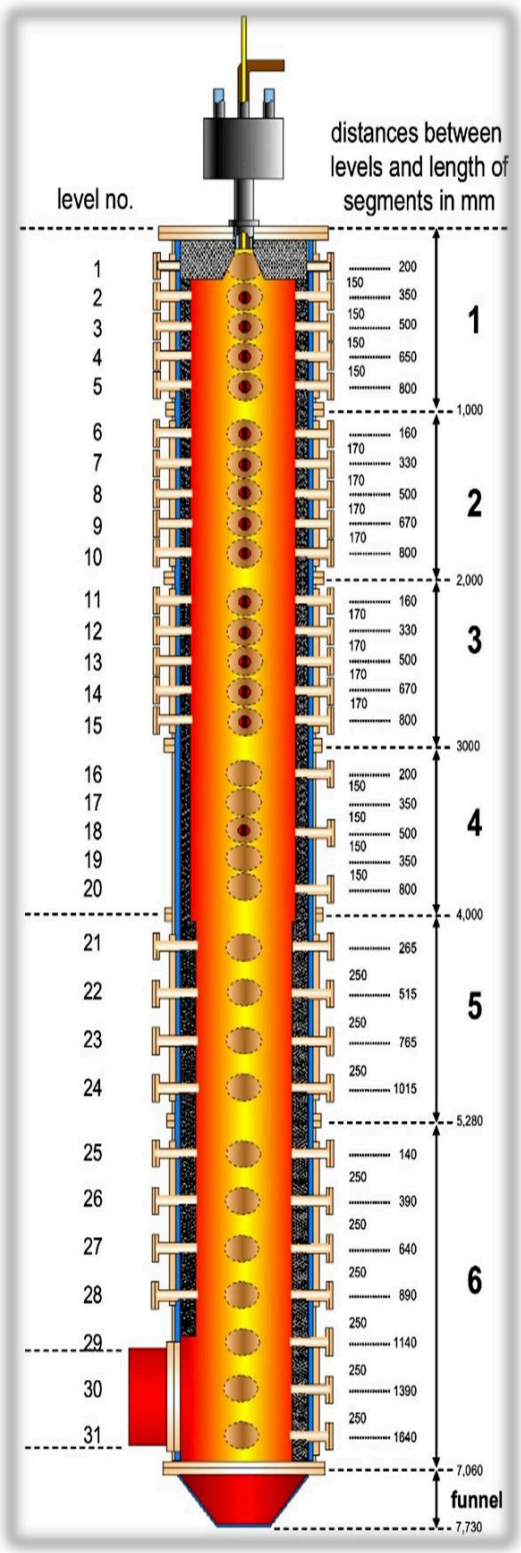

Figure 3.1 - KSVA test rig [52]

During the tests, temperature sensors were installed on levels 2, 3, 5, 6, 8, 10, 11, 13 and 15 to monitor the temperature profile during operation. For the measurement of the different gas emissions at the end of the combustion chamber, different gas analyzers were employed; infrared and ultraviolet sensors were installed at levels 7 and 11, respectively, which one

working on a different principle, Table 3.1 lists down the gas analyzers used for measuring gas emissions.

Table 3.1 - List of gas analyzers at KSVA

Emissions	Type of Analyzer
O2	Paramagnetic oxygen analyzer
CO, CO_2	Non-dispersive infrared spectrometer
NO, NO_2, SO_2	Ultraviolet process photometer

3.2 Description of the burner

The burner used in this parametric study is a pulverized swirl burner designed to create short flames lengths with high turbulence flow which is vertically attached to the top of the combustion chamber. Figure 3.2 sketches the vertically mounted burner.

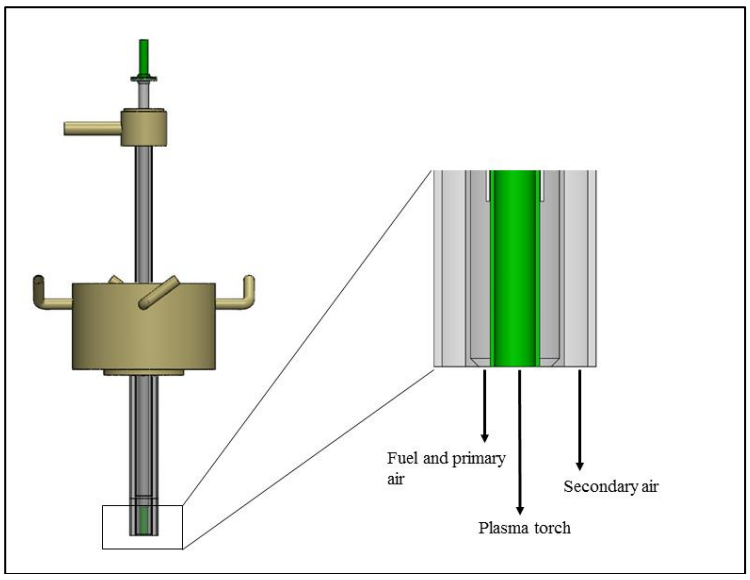

Figure 3.2 - Movable block swirl burner integrated with a plasma ignition system [53]

Primary air and fuel mixture are introduced to the furnace through the inner annulus of the burner, while the four inlets on the outer periphery allow for secondary air intake. The plasma torch is integrated into the burner, vertically inserted into the top central opening. The degree of swirling can be controlled by the moving the block swirler. Figure 3.3 shows the cross-sectional layout of the burner outlet.

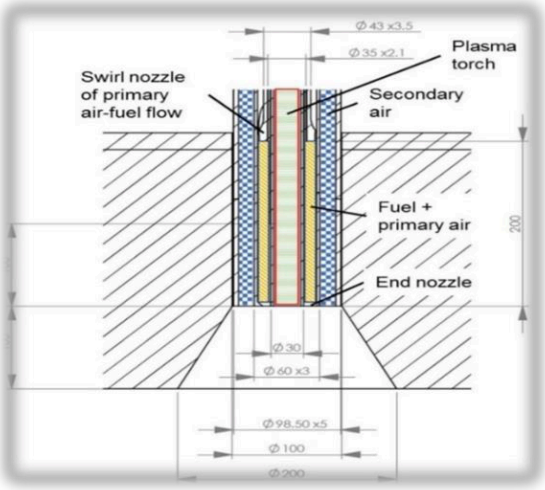

Figure 3.3 - Cross-sectional layout of the burner outlet [54]

During the measurement campaign, the plasma nozzle is set to a position of 0 mm between its end and the burner outlet, later, the plasma rod then is retracted inside the burner at -40 mm to observe the effect of the interaction of pulverized fuel mixture with the plasma flame at increased residence time. To achieve the position, an aluminum block with 40 mm of height was inserted between the plasma rod and the top of the burner, rising the end nozzle 40 mm. The block is then removed to achieve the plasma position “0 mm”.

3.3 Description of plasma system - PIAP

The plasma ignitor used in the study is the PIAP system, it utilizes DC current to create an arc and ionize air as carrier gas, obtaining a plasma flame with stable power that is able to reach high temperatures. As already mentioned in the previous section, the fuel, when passing through the plasma flame, rapidly release its volatiles and break down. Figure 3.4 shows the flame developed by the plasma system.

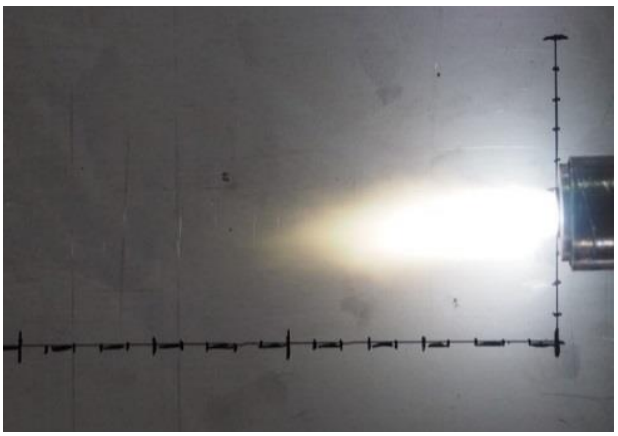

Figure 3.4 - PIAP plasma flame [51]

The output power can be controlled by adjusting the amperes provided and the amount of carrier gas flow through the generated arc. The thermal power employs a power factor (PF)

which accounts for the power losses on the system. The following equations illustrate the conversion between thermal and electrical power.

$$Eletrical\ Power\ (W) = Current\ (A)\ x\ Voltage\ (V) \tag{3.1}$$

$$Thermal\ Power\ (kW) = Eletrical\ Power\ (kW)\ x\ Power\ Factor \tag{3.2}$$

The velocity of the plasma jet is given by the following equation:

$$Velocity\ of\ Plasma\ jet\ \left(\frac{m}{s}\right) = \frac{\dot{V}\ Carrier\ gas\ flow\ \left(\frac{l}{min}\right)\ x\ 16.6}{\frac{\pi}{4}d^2\ (mm)^2} \tag{3.3}$$

The following table lists down the current, velocity and gas flow rate for different electrical powers of the PIAP system.

Table 3.2 - PIAP energy output

Current (A)	Voltage (V)	Carrier gas Flow $\left(\frac{l}{min}\right)$	Plasma Velocity $\left(\frac{m}{s}\right)$	Electrical Power (kW)
30	149	27	2.7-2.8	4.47

3.4 Description of the fuel

For this study, 6 mm pelletized wood was used, the fuel was pulverized, and different shares were generated to produce fuel samples. The physical and chemical properties of the fuel is explained in the following subsection.

3.4.1 Description of milling system and sieving machine

The pulverization of the fuel was done in-house in IFK's hammer mill machine with 1 mm mesh plates ensuring adequate milling. The fuel was fed at a constant rate to the machine, aiming to produce similar particle size distribution thru out the operation.

The procedure of sieving the raw pulverized fuel took place in order to produce different shares of particles to produce a number of samples with different particle size distributions. Sieve plates of 100 μm, 212 μm and 315 μm were used to sieve the raw pulverized fuel into different shares. Shares that were later mixed with raw fuel to create samples with particles size distribution of interest. Distinct samples were generated for this study, table 3.3 shows the code and description of each sample which will be used from now on.

Table 3.3 - Legend of generated samples

Samples	Observation
Raw fuel	Pulverized pelletized wood 1 mm
Sieved 100	Raw fuel sieved at 100 μm
Sieved 200	Raw fuel sieved at 212 μm
Sieved 300	Raw fuel sieved at 315 μm
Mix 100	30 kg of raw fuel + 100 μm fine share
Mix 200	30 kg of raw fuel + 212 μm fine share
Mix 300	30 kg of raw fuel + 9 kg of 315 μm fine share

3.4.2 Particle size distribution analysis

A physical analysis of the fuel was conducted in-house, two methods were applied, the first particle size distribution (PSD) was done in a mass basis and the second method was done in a volumetric basis.

The mass basis method follows the standard testing procedure ASTM B214-07 [55] dry sieving analysis, which is suitable to determine the PSD of mixed powders with particles sizes ranging from 45 to 1000 μm. All the different samples were analyzed at the same test conditions and the resulting cumulative PSD curves are presented in Figure 3.5.

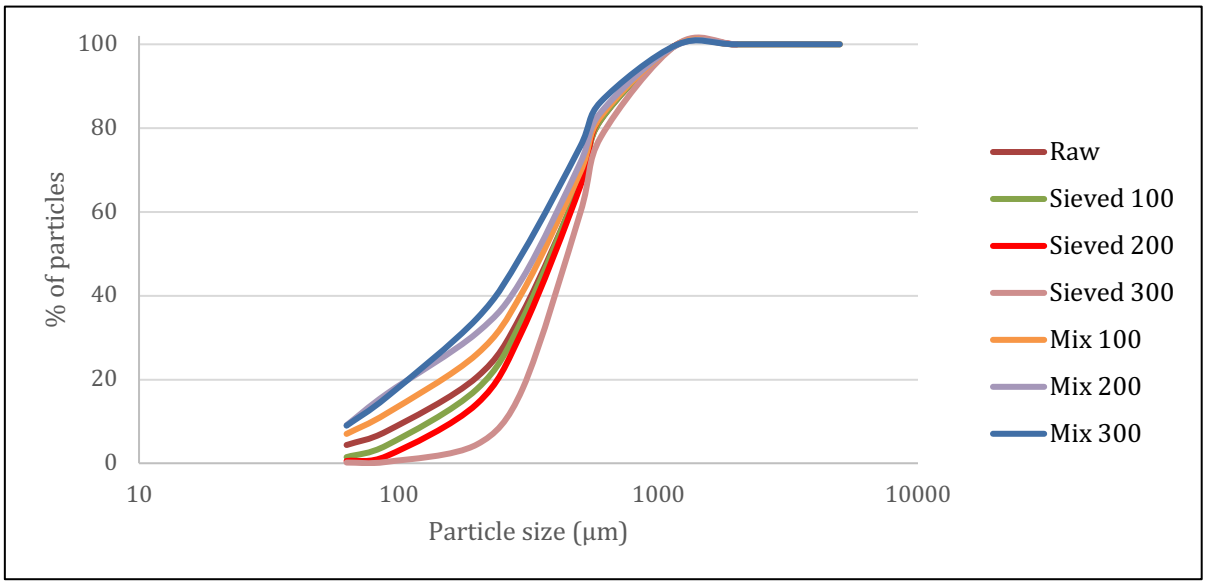

Figure 3.5 - Cumulative size distribution - Mass basis

The second method consisted of utilizing the "Malvern Instruments Mastersizer 3000" device for measuring the PSD in fuel samples. Using laser diffraction technology, the particles are scattered in the air and the samples are passed through a laser beam. Once the particle is inside the beam, the laser is diffracted, and the different intensities (based on angular variation) of the diffracted source which is a function of the size of particles is obtained.

Through this principle of particle size measurement, two characteristics curves, cumulative size distribution and distribution density, in a volumetric basis can be obtained.

It is relevant to notice that as the milling process produces a series of different particles shapes and sizes, it was important to define on the device that the analyzed particles had in its majority spherical or non-spherical shapes, through that, was possible to obtain a more accurate analysis. Both spherical and non-spherical cumulative size distributions curves are presented in Figure 3.6 together with the mass PSD for the pulverized pelletized wood raw sample, and as is possible to notice, that both curves are overlapped, but the spherical assumption curve maintains itself closer to the mass PSD, behavior that was seen in all the other samples, more results and comparisons can be found in Appendix A – PSDs.

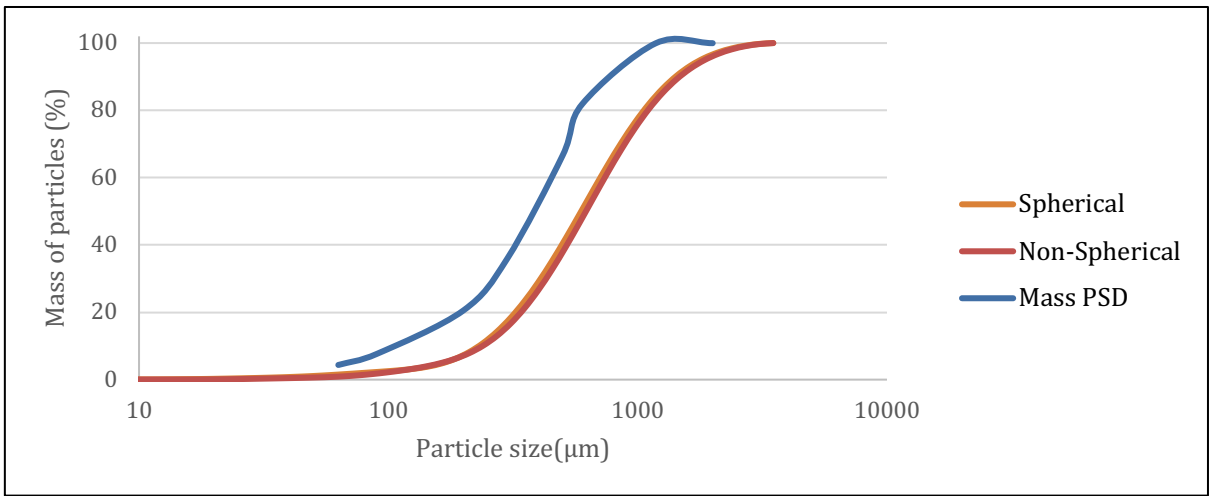

Figure 3.6 - Cumulative size distribution - Pulverized Raw fuel sample

The PSD for the pulverized biomass raw sample is presented in Figure 3.7, both spherical and non-spherical assumptions are shown.

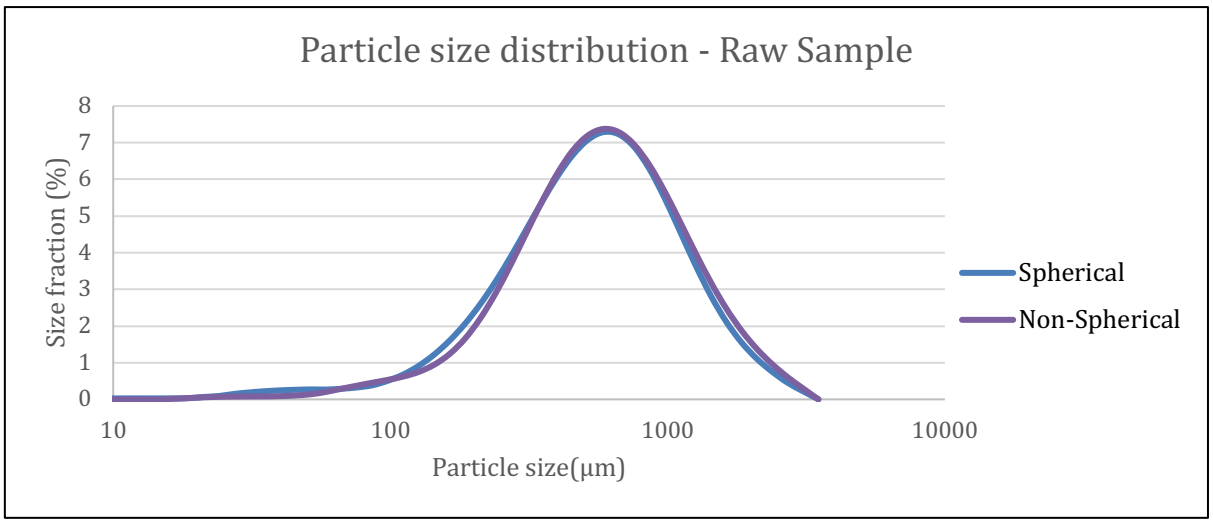

Figure 3.7 - Particle size distribution - Pulverized Raw fuel sample

Three characteristic diameters D10, D50, D90 are also obtained from the cumulative size distribution curve, D50 is the median diameter that represents 50% of the sample which has a

diameter less than D50. Similarly, D10 and D90 represent the diameters at which 10% and 90%, respectively, of the sample diameters smaller than D10 and D90. The values of these characteristic diameters presented in Table 3.4 for the raw fuel sample.

Table 3.4 - Characteristic diameters - Pulverized Raw Fuel sample

D	Raw – Mass PSD (μm)	Raw – Spherical (μm)	Raw – Non-Spherical (μm)
D10	109.99	149.18	198.04
D50	391.69	547.54	567.45
D90	860.57	1349.83	1404.62

Table 3.5 presents the different volumetric analysis characteristic diameters for each sample; for method of comparison, only the spherical assumption was considered, as mentioned before. As expected, the samples produced a finer share distribution, as the sieved samples produced a coarse share. This difference influences the ignition behavior and will be discussed in the results section.

Table 3.5 - Characteristic diameters - Volumetric analysis

D	Raw (μm)	Sieved 100 (μm)	Sieved 200 (μm)	Sieved 300 (μm)	Mix 100 (μm)	Mix 200 (μm)	Mix 300 (μm)
D10	149.18	198.06	253.04	327.96	82.42	67.92	69.97
D50	547.54	598.28	621.83	702.09	440.06	467.38	362.55
D90	1349.83	1570.22	1405.60	1494.25	1024.81	1392.11	960.12

3.4.3 Chemical analysis

The chemical analysis of the fuels was performed in-house in IFK according to the standard procedures and conditions. The proximate analysis was done according to DIN 51718, 51719 and 51720, while the ultimate analysis was done according to DIN ISO 10694. The details of the analysis and their procedures can be found in the mentioned literature. The results of the analysis are mentioned below in Table 3.6 and Table 3.7 according to as received (a.r) basis. It should be considered that carbon content in the proximate analysis is not directly measured. it is calculated by subtracting the percentage of ash, volatile matter and moisture from 100 %; similarly, the oxygen content in the ultimate analysis is calculated by subtracting the percentage of other elements from 100 %.

Table 3.6 - Proximate analysis - Raw fuel

Proximate analysis	a.r	w.f.
Moisture Analysis (%)	5.70	-
Volatile Content (%)	76.8	81.5
Ash (O_2 + 815 °C) (%)	0.10	0.11
Fixed Carbon (calc.) (%)	17.4	18.4

Table 3.7 - Elemental analysis - Raw fuel

Elemental analysis	a.r.	w.f.
Carbon (%)	48.0	50.9
Total hydrogen ($H_{tot.}$) (%)	6.46	6.18
Total hydrogen ($H_{org.}$) (%)	5.82	6.18
Nitrogen (%)	0.193	0.205
Sulfur (%)	0.058	0.062
Chlorine (%)	0.031	0.032

The calorific value was determined in-house in IFK by using Calorimeter IKA C 4000. DIN 51900 standards were followed. Table 3.8 lists down the calorific values of each fuel.

Table 3.8 - Calorific analysis - Raw fuel

Component	a.r.	w.f.
Gross Calorific Value ($J \cdot g^{-1}$)	18 794	19 930
Net Calorific Value ($J \cdot g^{-1}$)	17 388	18 586

3.5 Calibration of fuel feeder

A Screw extruder with an attached dispersing chamber is used to control the feed the fuel to the burner chamber through mass transport phenomena. The fuel particles are dispersed in the container and transported via carrier air. The amount of fuel transported to the burner is governed by the rotating frequency of the screw which feeds fuel to the chamber.

The calibration was done by calculating the mass flow rate of the raw fuel against five different inputs current of the screw controller, and a co-relation was developed. For each current, the biomass was fed for 1 minute, and the extruded fuel was carefully weighted; the calibration test was repeated at least one more time for each frequency to ensure reproductivity of results, and a correlation between rotation frequency and the mass flow rate was developed. The coefficient of determination indicates an error of less than 0.001%. Hence, after successful calibration, the experiments were carried out using the characteristic equation listed on the following

Figure 3.8.

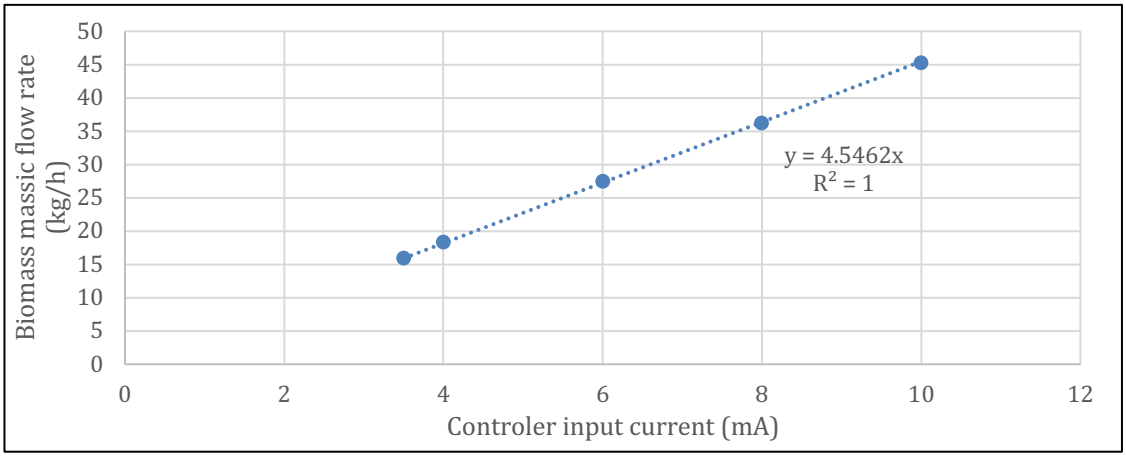

Figure 3.8 - Calibration curve of the Screw feeder

3.6 Parametric study layout and data collection

After final preparation of the facility, different operational parameters are defined focusing to observe the influence of wood pellets particle size on plasma-assisted ignition. The plasma electrical power is kept constant for all tests, at 4.47 kW with, Equation (3.2) and assuming an power factor of 0.7, the approximate plasma thermal output is of 3.0 kW_{th}; to study the effect of the thermal load, the fuel mass flow rate variated to provide thermal outputs of 100 kW_{th} to 300 kW_{th}; for the effects of different air-fuel ratio (lambda), the primary air flow is kept constant at 30 Nm^3/h, and the secondary air flow to the burner is adjusted in each test to achieve sub-stoichiometric conditions of lambdas as low as 0.5, to excess air conditions of lambda 1.1. The study of the iteration effect between primary air-fuel mixture with the plasma flame is done by retracting the plasma ignitor from “0 mm” to “-40 mm”, as explained in section 3.2. The thermal load and airflow can be adjusted through KSVA control room, while the change on the ignitor position has to be done locally. The following Table 3.9 summarizes the studied parameters for each sample. An example of the test matrix which was used to guide though out each battery of tests can be found in Appendix A – Test Matrix.

Table 3.9 - Studied parameters

Parameters	Variation
Thermal load	100 kW_{th}, 125 kW_{th}, 150 kW_{th}, 200 kW_{th}, 250 kW_{th}, 300 kW_{th}
Lambda	0.4, 0.5, 0.6, 0.7, 0.9, 1, 1.1
Plasma position	"0 mm" and "-40 mm"

During the course of the measurement campaign, the following standards were followed to keep consistency in all tests: Before the beginning of each test, the combustion chamber had to be cooled down below 90 °C to simulate cold start-up conditions. The test begins at the moment the plasma system is turned on; the fuel feeder is started 10 seconds after. The plasma system is turned off 30 seconds after ignition, the test is terminated after evaluating the flame stability; if during the plasma ignition step blow out occurs, the test is terminated; if no ignition

is seen when the fuel feeder is turned on, the test is terminated. CO, CO_2, and NOx emissions released during each test were measured continuously and the data recorded. For safety, CO emissions were allowed to reach concentration below 200 ppm before the next test was performed. The facility was thoroughly cleaned after concluding the test matrix for each sample, and the facility is prepared for the next battery of tests.

3.7 Methods of evaluation

Two methods of evaluation were used to evaluate the data obtained from combustion tests:

1. Quantitative data evaluation
2. Qualitative flame evaluation

3.7.1 Quantitative data Evaluation

As presented in the literature review, the major step governing the ignition and combustion of biomass is the devolatilization and formation of a combustion front where oxygen diffuses through the particle. Hence, the extent of combustion degree achieved in each test was evaluated by calculating the percentage of consumed oxygen 30 seconds after the ignition occurs.

The combustion degree is calculated using equations 3.4-3.8. Since the consumed amount of oxygen during each test is known, it's possible to estimate the amount of biomass which ignited, and by comparison with the fuel flow rate, the combustion degree can be obtained. Relevant findings are discussed in the results and discussion section of this study.

During the test, the O_2 in the combustion chamber is being constantly measured, by Equation 3.5, is possible to obtain the specific amount of volumetric O_2 which was consumed, and assuming complete combustion, the minimum oxygen demand can be calculated by Equation 3.6.

$$\Delta_{O_2} = O_{2,t0} - O_{2,t1} \tag{3.4}$$

$$\dot{V}_{consumed\ O_2}\left(\frac{m^3{}_N}{h}\right) = \Delta_{O_2} \cdot \dot{V}_{TA}\left(\frac{m^3{}_N}{h}\right) \tag{3.5}$$

$$O_{min,dry}\left(\frac{m^3_{N,O2}}{kg_{fuel}}\right) = O_{min,CO2}\left(\frac{m^3_{N,O2}}{kg_C}\right)\cdot c_C + O_{min,H2O}\left(\frac{m^3_{N,O2}}{kg_H}\right)\cdot c_H + O_{min,SO2}\left(\frac{m^3_{N,O2}}{kg_S}\right)\cdot c_S - O_{min,O2}\left(\frac{m^3_{N,O2}}{kg_O}\right)\cdot c_O \tag{3.6}$$

$$\dot{M}_{consumed\ fuel}\left(\frac{kg}{h}\right) = \frac{\dot{V}_{consumed\ O_2}\left(\frac{m^3{}_N}{h}\right)}{O_{min,dry}\left(\frac{m^3_{N,O2}}{kg_{fuel}}\right)} \tag{3.7}$$

$$Combustion\ degree\ (\%) = \frac{\dot{M}_{consumed\ fuel}\ \left(\frac{kg}{h}\right)}{\dot{M}_{f}\ \left(\frac{kg_{fuel}}{h}\right)} \cdot 100 \tag{3.8}$$

3.7.2 Qualitative data evaluation

In addition to the quantitative data evaluation of each test, a qualitative combustion class by visual observation is also characterized. The following table lists down the combustion classes and its definition which was assigned for all the tests. Equation 3.8 will be used in combination with the combustion classes to propose suitable boundary conditions for biomass combustion with assisted plasma ignition.

Table 3.10 - Classification of the ignition and combustion behavior by visual observation

Combustion Class	Definition
0	No Ignition
1	Ignition and fast extinction (only sparks)
2	Ignition and unstable flame with plasma
3	Ignition and stable flame with plasma
4	Ignition and extinction in few seconds without plasma
5	Ignition and detached flame without plasma
6	Ignition and attached flame without plasma

4 Results and discussion

The following section discusses the results from the measurement campaign obtained by the variations of the different operational parameters defined in section 3. To discuss the combustion behavior of a given sample against a specific operational parameter, all other parameters must be kept constant. For the uniformity of the results, the primary air flow was kept constant at 30 Nm^3/h and the burner secondary air swirling mechanism is kept at maximum. Only the most prominent and relevant results are presented. A techno-economic assessment with costs to retrofit the plasma system in an existing power plant is also presented; the results section is organized as follows:

1. Effect of thermal load;
2. Effect of air-fuel ratio;
3. Effect of plasma position;
4. Comparison of the different fuel samples;
5. Techno-economic assessment.

After discussing and observing the behavior of each sample and conditions for ignition against all the operational parameters, suitable boundary conditions for biomass combustion with assisted plasma ignition are proposed.

4.1 Effect of thermal load

The following sub-section illustrates the results obtained by variating the thermal loading on each sample with different lambdas. Increasing the thermal load brings a higher amount of fuel and oxygen available for ignition and combustion; this results in a better devolatilization and improved reaction kinetics.

Table 4.1 lists down the experimental settings used for investigating the effects of thermal load; for methods of comparison only a few settings will be discussed in this subsection; more will be discussed later on.

Table 4.1 - Thermal load effect - Experimental settings

Parameters	Setting
Tested thermal loads (kW_{th})	100, 125, 150, 200, 250
Maximum thermal Load (kW_{th})	500
Lambda	0.5, 0.6, 0.7, 0.9, 1.1
Plasma power (kW)	4.2
Plasma position	"0 mm"

Figure 4.1 illustrates the results obtained with the Raw sample; the figure describes the effect of increasing thermal load on sub-stoichiometric conditions for lambdas 0.5, 0.7 and 0.9. At 20% thermal load, unstable ignition is observed for lambdas 0.7 and 0.9, lambda 0.5 was not tested as the other sub-stoichiometric conditions didn't produce stable flame. By increasing the thermal load to 25%, there is a slight improvement in combustion degree, it was possible to obtain stable flame, but only with the plasma on, the combustion degree was less the 10% for both cases. Thermal loads of 30% and 40% resulted in an increase of combustion degree, all cases showed at least an ignition class number 3; it's important to notice that at 40% thermal load, combustion degree was smaller than the trend, its believed that as it was the first tests of the day, the furnace walls were at room temperature which produce a worse combustion degree result, even though all the other tests it was waited for the furnace reach temperatures less then 90 ºC, this difference even if small, it is relevant, which reflected on the discrepancy. Further increasing the thermal load to 50%, there is a proportionate rise on the combustion degree, following the trend, as expected; this is explained by the fact that an increase in thermal load increases the amount of fuel that interacts with the plasma flame. Hence, a higher devolatilization is achieved with increased combustion degree.

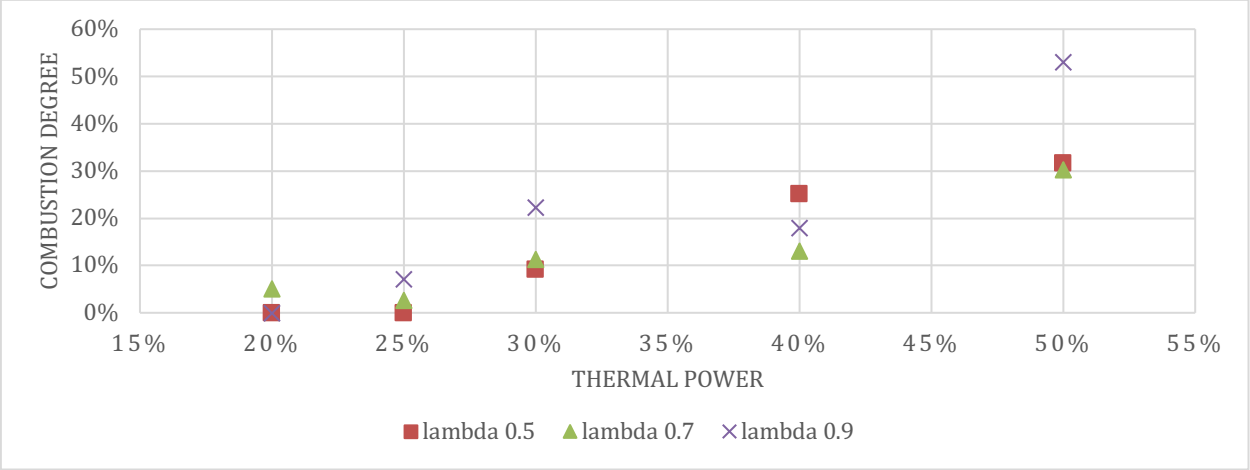

Figure 4.1 - Effect Thermal load - Raw sample

Figure 4.2 shows the results for mix 100 sample, the figure outlines the effect of increasing thermal load on sub-stoichiometric conditions lambdas 0.7, 0.9 and excess air lambda 1.1. At 25% thermal load it's possible to observe with this fuel a slight improvement on the combustion degree, when comparing with the previous one, which is relevant since there was an increase of particles bellow 100 μm, but more on the fuel comparisons will be discussed later on. At 30% it's possible to notice that sub-stoichiometric conditions produced inferior combustion degree then in excess air; in those situations where the result doesn't follow the trend, is always possible to see two peeks in O_2 consumption, as we are only considering the peek 30 seconds after ignition, the result shows a smaller combustion degree; this happens because during ignition, there will be a lack of O_2, the flame will diminish, and then starts to increase again, Figure 4.3 illustrates this behavior, it was possible to identify combustion class 4 in several tests. Reaching 40% and 50% of thermal load there is the proportional rise in combustion degree as seen previously, sub-stoichiometric conditions created flames class 4 and class 6, where excess air conditions had a class 3 type of flame, an increase of air velocity at lambda 1.1 leads to higher thermal losses, reducing the combustion degree.

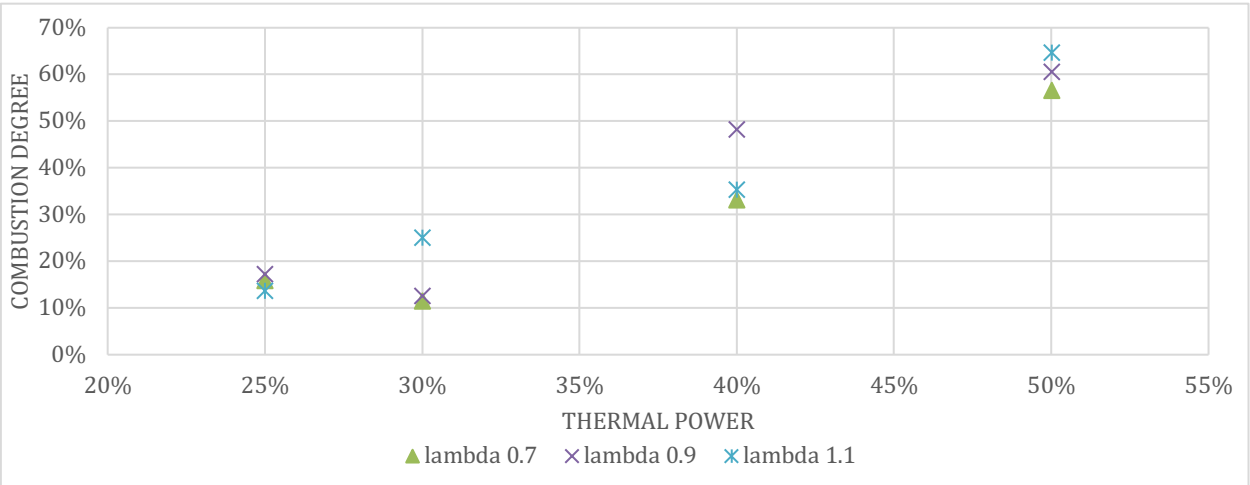

Figure 4.2 - Effect thermal load - Mix 100

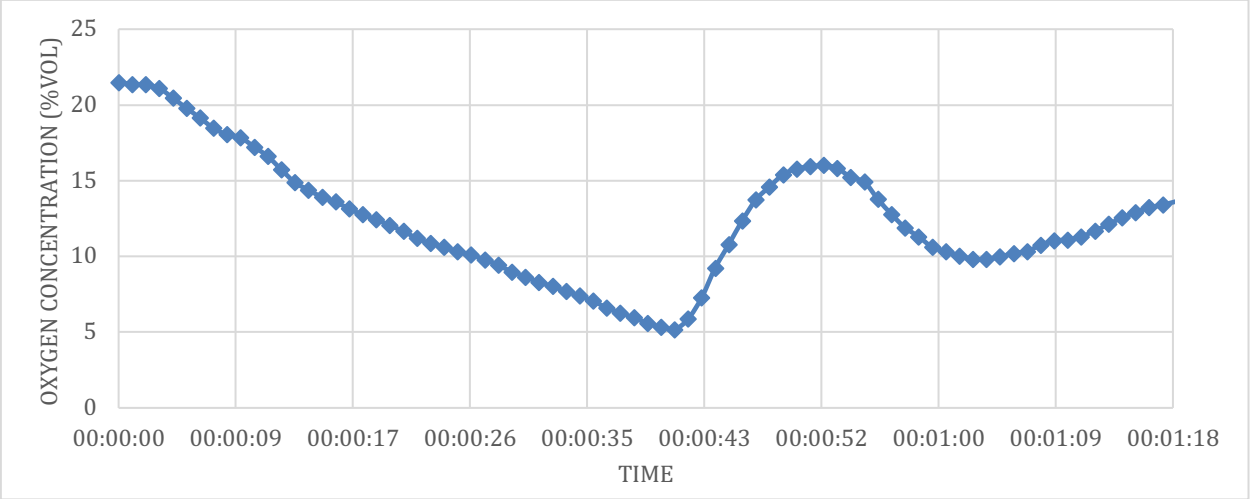

Figure 4.3 - O_2 consumption - Mix 100 - 200 kW - lambda 0.9

Figure 4.4 illustrates the results for mix 200 sample, the figure outlines the effect of increasing thermal load on sub-stoichiometric conditions lambdas 0.7, 0.9 and excess air lambda 1.1. At 20% thermal load, only lambdas 0.7 and 0.9 are considered, as they were the only settings which produced combustion class type 3, the combustion degree was less then 5 % for both; it can be presumed that sufficient devolatilization was not achieved, hence a smaller combustion degree. Increasing to 25% thermal load it's possible to observe an increase in combustion degree as the quantity of finer share which interacts with the plasma flame increases, with that a better ignition. At 30%, 40% and 50% thermal power follows the same trend as expected, with a special attention for lambda 1.1 at 40% thermal power which had two O_2 combustion peeks, hence a smaller combustion degree; both 40% and 50% thermal load presented combustion class of 6 in almost all cases, except for lambda 1.1 where the combustion class was type 4.

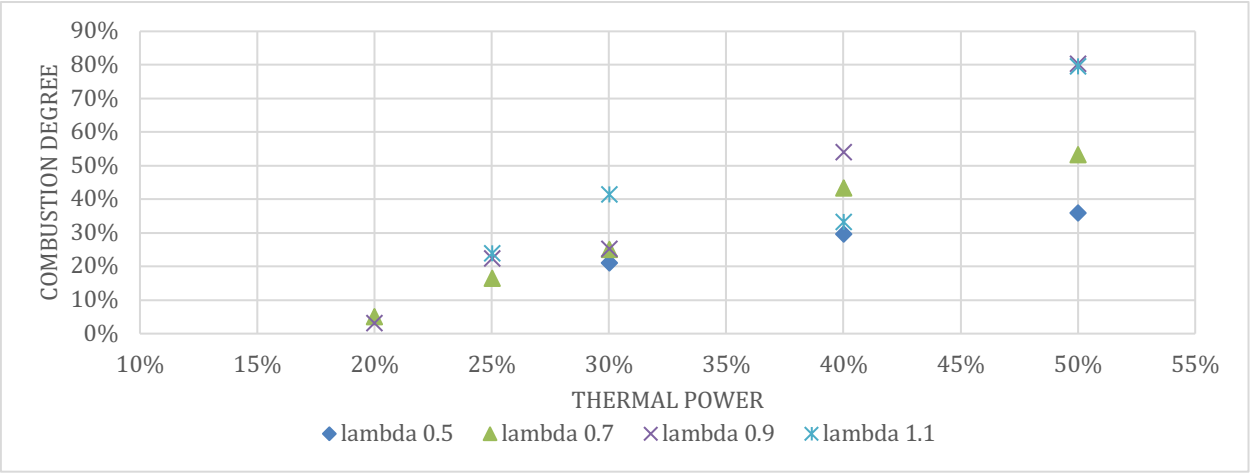

Figure 4.4 - Effect thermal load - Mix 200

Figure 4.5 shows the results for mix 300 sample, effect of increasing thermal load on sub-stoichiometric conditions lambdas 0.7, 0.9 and excess air lambda 1.1 are considered. It's possible to notice an enhance on the combustion degree when compared to previous fuel

samples, as this sample has the greater quantity of finer particles which are not only responsible for the first ignition, but also for maintaining the flame. At 20% thermal load, there was ignition with combustion class type 4; increasing to thermal loads of 25% and 30% there is a slight increase in the combustion degree; 40% and 50% burner load present the best combustion degree.

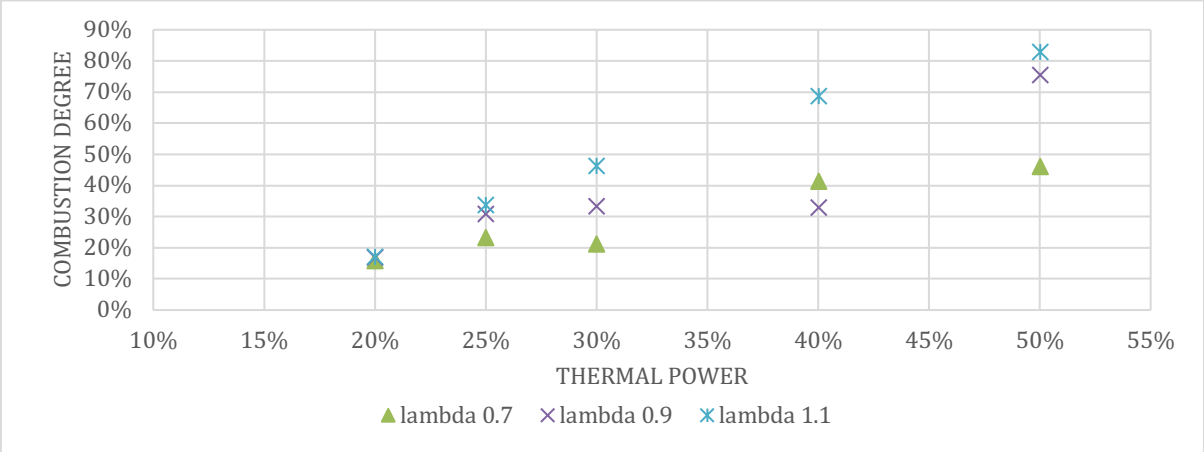

Figure 4.5 - Effect thermal load - Mix 300

4.2 Effect of air-fuel ratio

In this subsection, the effect of air-fuel ratio (lambda) will be discussed on different fuel samples used in this study. Since primary air is kept constant during all tests, increasing the air-fuel ratio increases the amount of secondary air available, increase which means more O_2 available for the fuel which improves the combustion reaction kinetics. Increasing the secondary air also promotes the collision of molecules and intensifies the turbulent mixing of air and fuel particles which promotes better combustion with intense flame re-circulation zone at the exit of the burner. However, increasing the air-fuel ratio also increases the velocity of the air; excessive air velocity increases the heat losses to the walls of the combustion chamber, phenomena which will be discussed in the following results.

The effect of air-fuel ratio is discussed on two thermal loads 150 kW_{th} and 250 kW_{th} since the first one has a representing behavior at 30 % burner load, where the second corresponds to 50 % of the thermal load. Table 4.2 lists down the experimental settings used to investigate the effect of air-fuel ratios.

Table 4.2 - Effect air-fuel ratio

Parameters	Setting
Tested burner loads	30 %, 50 %
Maximum thermal Load (kW_{th})	500
Lambda	0.5, 0.6, 0.7, 0.9, 1.1
Plasma power (kW)	4.2
Plasma position	"0 mm"

Figure 4.6 illustrates the combustion degree results for the raw sample on different lambdas. At lower 30% thermal load it is seen that increasing the lambda from 0.5 to 0.7 didn't affect the combustion degree in an overall manner, which brings into question if the increase in air-fuel ratio is increasing the heat losses at similar rate which is affecting the combustion degree, further increasing lambda to 0.9 is possible to observe an slight increase in the combustion degree, the increase in air flow leads to an increase in turbulent mixing which positively affects the combustion degree. At 50% thermal load is possible to notice the heat loss effect between lambdas 0.5 and 0.7, as there is a slight decrease in the combustion degree, while at lambda 0.9 there is an increase in combustion degree as seen at 30% thermal load.

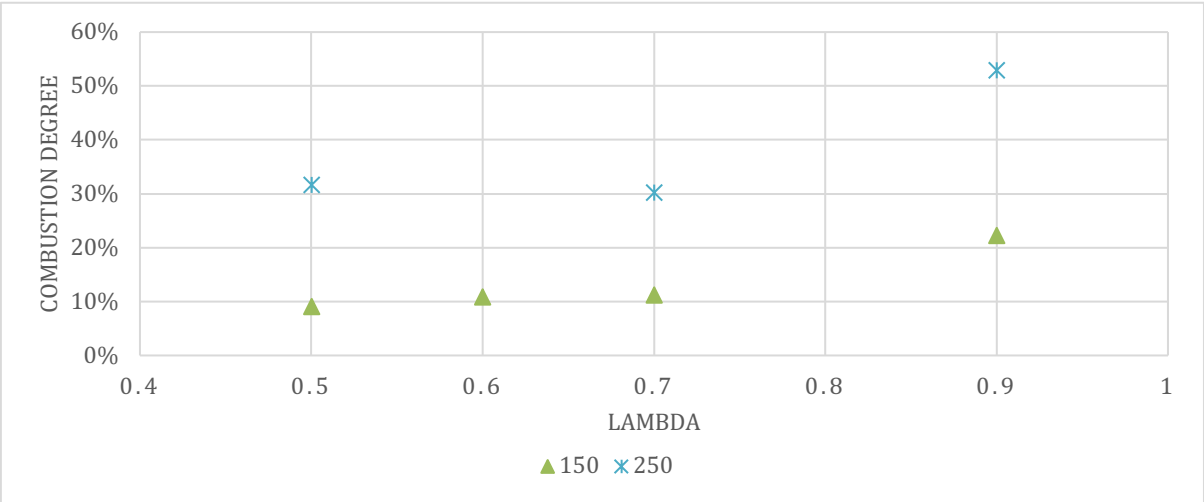

Figure 4.6 - Effect air-fuel ratio - Raw sample

Figure 4.7 shows the combustion degree results for the mix 100 sample on different lambdas. At lower 30% thermal load is possible to notice that the behavior is consistent as the previous sample, where there is a higher increase at lambda 1.1, which means that the heat production from the flame overcame the increase in heat loss to the furnace wall. At 50% thermal load, there is an increase in combustion degree between lambdas 0.5 and 0.7, the increase in the fuel finer share may be responsible for this slight increase, as there is an increase in the

turbulent mixing with an higher air flow, more particles which are responsible for the first ignition interact with the plasma flame. Continuing to increase the air to fuel ratio to values of 0.9 and 1.1 there is an increase in the combustion degree, but as the secondary air is further increase, the heat loss effect starts to increase due to excess air velocity.

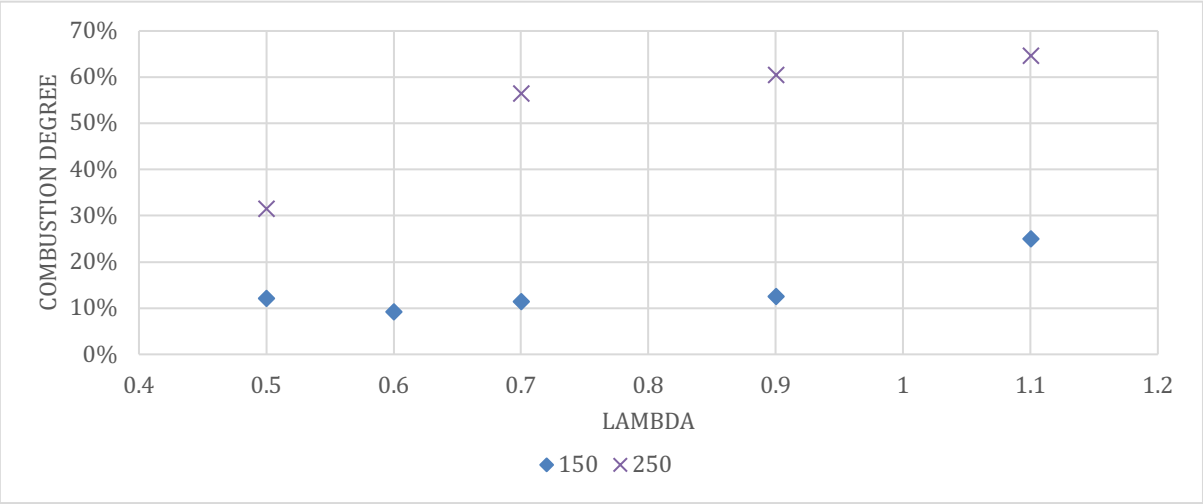

Figure 4.7 - Effect air-fuel ratio - Mix 100

Figure 4.8 and Figure 4.9 presents the effect of air fuel ratio for the mix 200 and mix 300 samples, both fuels behaved similarly at the same settings. At 30% thermal load, following the behavior from the first two fuels, between lambdas 0.5 and 0.7 the combustion degree maintains the same, with an increasing combustion degree at lambda 1.1. At 50 % thermal load, there is an increased combustion degree rate as lambda increases from 0.5 to 0.9, while at lambda 1.1 the combustion degree stagnates as the heat loss effect starts to dominate due to excess air velocity.

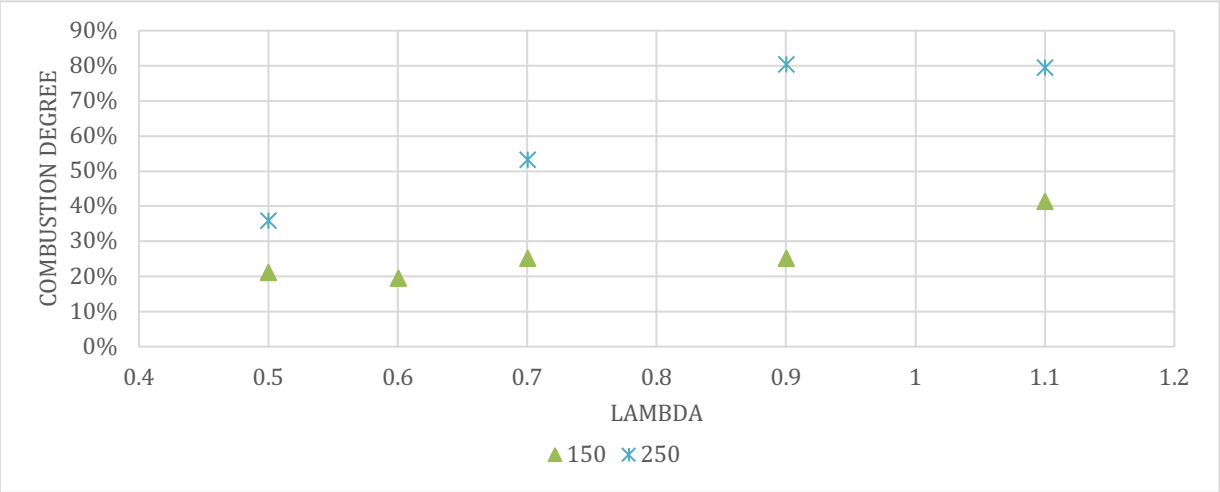

Figure 4.8 - Effect air-fuel ratio - Mix 200

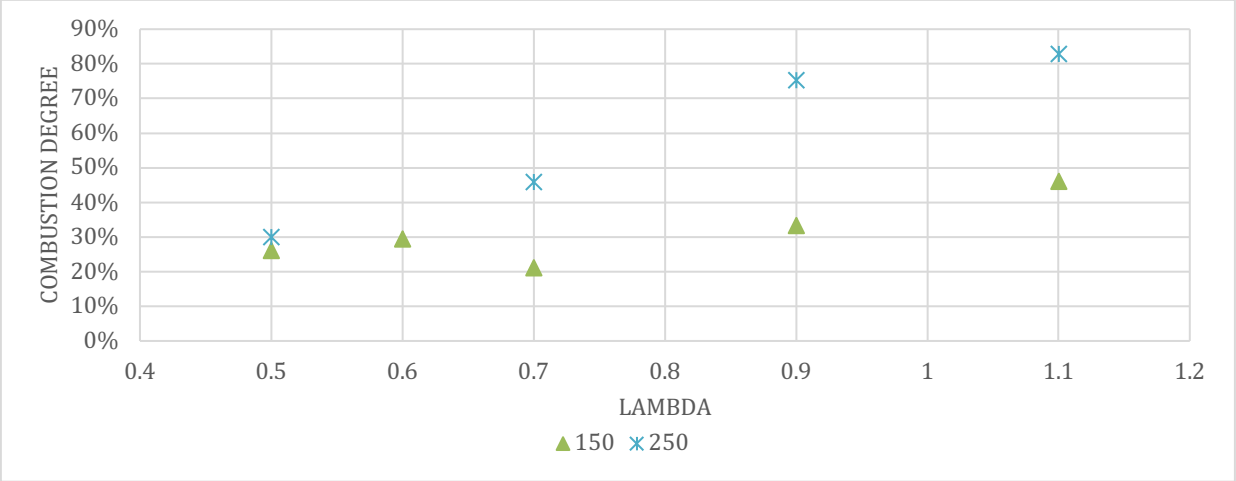

Figure 4.9 - Effect air-fuel ratio - Mix 300

4.3 Effect of plasma position

In this subsection, is discussed the effects of the plasma ignitor position based on the retraction of the plasma torch to "-40 mm" position in comparison to the normal position "0 mm". By moving the plasma position to "-40 mm", the interaction between the fuel and the plasma flame happens in a confined area on the absence of secondary air, with that the residence time is increased. These effects are believed to improve the fuel-plasma interaction and are expected to increase the combustion degree.

Retracting the plasma torch may also bring some disadvantages, as is changed to the "-40 mm", the plasma flame is generated closer to the guide-vanes of the primary fuel-air mixture; these vanes resolve the flow into longitudinal, radial and axial directions to create turbulence and a swirling flow, the swirling of the fuel results in an alteration in the radial particle distribution; the particles are expected to be accumulated at the outer tube wall and therefore, affecting the fuel-plasma interaction.

Table 4.3 lists down the experimental settings used to investigate the effect of the plasma torch position:

Table 4.3 - Effect plasma position

Parameters	Setting
Tested thermal loads (kW_{th})	150, 200, 250
Maximum thermal load (kW_{th})	500
Lambda	0.5, 0.7, 0.9
Plasma power (kW)	4.2
Plasma position	"0 mm" and "-40 mm"

Figure 4.10 illustrates the effect of plasma position for the raw sample at lambda 0.7, since this is the setting with the most data points and wider representing behavior. At 30% thermal load ignition is only observed for position “0 mm”, further increasing to 40% thermal load, is possible to evidence unstable ignition at position “-40 mm”, neither the less the low share of fine particles is believed to be responsible for the poor performance of this fuel sample; the finer fuel particles are accumulated at the outer tube wall as the radial particle distribution restrict the fuel-plasma interaction, resulting in a weak ignition.

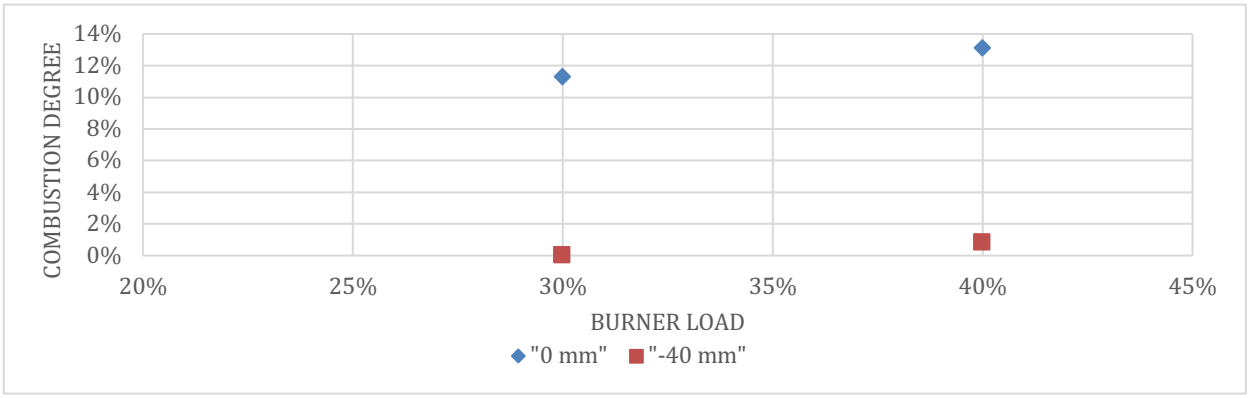

Figure 4.10 - Raw sample - Lambda 0.7

Figure 4.11 shows the effect of plasma position for the mix 100 sample at setting lambda 0.7. At 25% thermal load ignition is only seen at position “0 mm”, but by further increasing the thermal load to 30%, the imperfect fuel-plasma interaction caused by primary air guide-vanes is overcome by the higher amount of fuel available; hence, an increased residence time of the fuel in the plasma flame brings a positive effect of retracting the plasma torch as a better combustion degree is obtained, the same positive effect is seen at 40% thermal load.

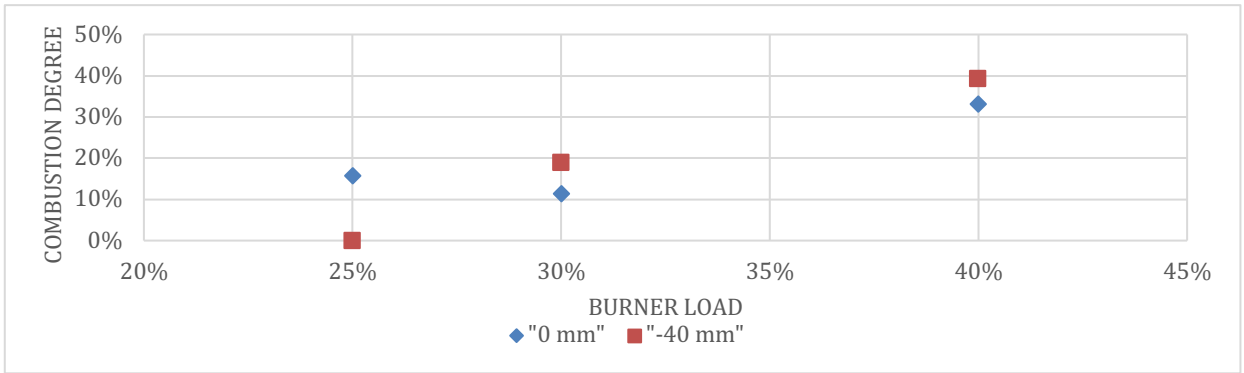

Figure 4.11 - Mix 100 - Lambda 0.7

Figure 4.12 and Figure 4.13 presents the effect of plasma position by increasing the thermal load at the same conditions for the mix 200 and mix 300 samples, the behavior is similar to the one seen with mix 100 sample, by increasing the amount of fuel, the imperfect interaction between the fuel and plasma is overcome and stable ignition is obtained.

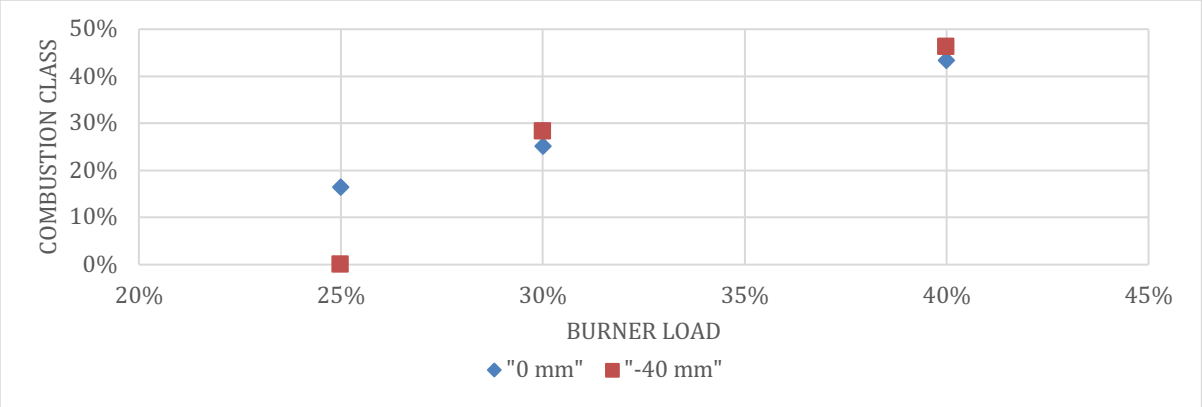

Figure 4.12 - Mix 200 - Lambda 0.7

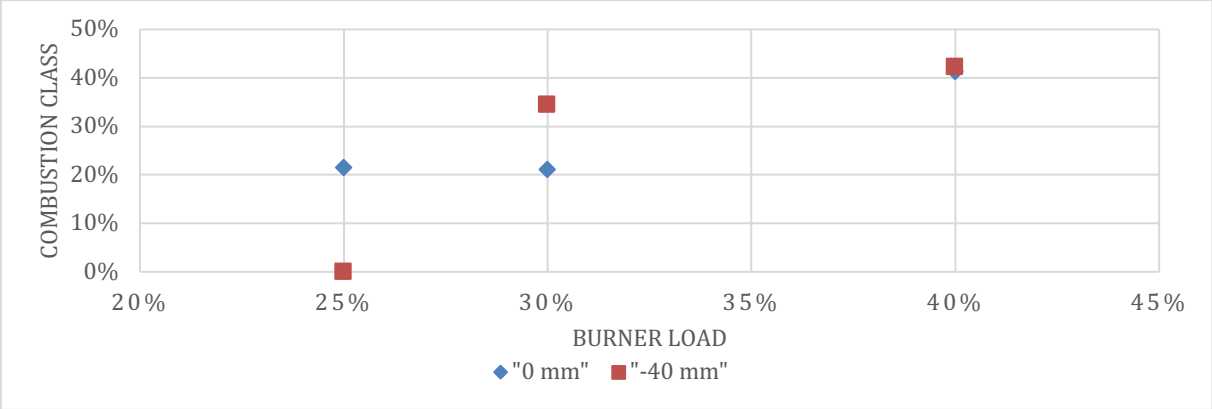

Figure 4.13 - Mix 300 - Lambda 0.7

4.4 Comparison of the different fuel samples

After comparing the combustion degree results and the combustion class assigned to each test against the different operation parameters, the fuels are compared together to investigate the influence of particle size. From all prepared samples, sieved 100, sieved 200 and sieved 300 were not taken into discussion in the previous subsections as in none of the tests ignition occurred, in spite of that, they are important, as these fuel samples define the turning point where ignition starts to occur. Following table lists down the experimental settings used to compare different fuels.

Table 4.4 - Fuel comparison parameters

Parameters	Settings
Thermal loads (kW_{th})	150, 200, 250
Samples	Raw, sieved 100, sieved 200, sieved 300 mix 100, mix 200, mix 300
Lambda	0.7
Plasma power (kW)	4.2
Plasma position	"0 mm"

Starting with the unsatisfactory fuels, sieved 300 had the worse behavior from all tested samples, sieving the finer share prevented the plasma flame from igniting the fuel, combustion class type 0 was assigned to all tests with this sample, this is an important result as defines that all particles bellow 300 μm will be responsible for the first ignition. Moving to sieved 200, the second worse fuel, it only was able to present a combustion class type 2, looking back at the PSD, there is a significant increase on the 100 μm – 300 μm share, difference which can account for the sparks seen during the tests, as the plasma flame is able to ignite smaller fuel particles, but not enough to achieve stable ignition. At sieved 100, the combustion class was type 2 at 50% thermal load; the share smaller the 100 μm was increased from less than 2% to 4%, but still not enough to achieve the critical value to stable ignition.

For the Raw sample, and the mix ones, the finer share of particles smaller the 100 μm was always higher than 8%, the double then sieved 100, difference which can define the critical share for stable ignition. Figure 4.14 illustrates the comparison of ignition performance between the different tested fuel samples at lambda 0.7. At 20% thermal load no ignition is observed for the raw sample and mix 100, as mix 200 and mix 300 already show combustion at this thermal load, further increasing the thermal load to 25% is possible to observe stable ignition in all four samples, so the point here is what changed when compared to 20 % thermal load, which makes this difference; when increasing the thermal load, in one hand, the fuel flow increases, which means more particles available to be combusted, but in the other hand there is also an increase within the secondary air flow, in this case 21%, which could account for the difference between thermal loads, as there is an improve in the turbulent mixing of fuel and air, which promotes combustion. Further increasing the thermal load to 30% and 40% there is a trend increase with all fuels as expected, but when reaching 50% thermal load, there is a slight decrease of the mix 300 combustion degree, the hypothesis is that as the secondary air flow is higher, the finer share doesn't has enough residence time within the plasma flame to ignite, which could be another point that supports the idea to retract the plasma torch to "-40 mm" position in this case to increase the residence time within the plasma flame, as discussed in the previous subsection.

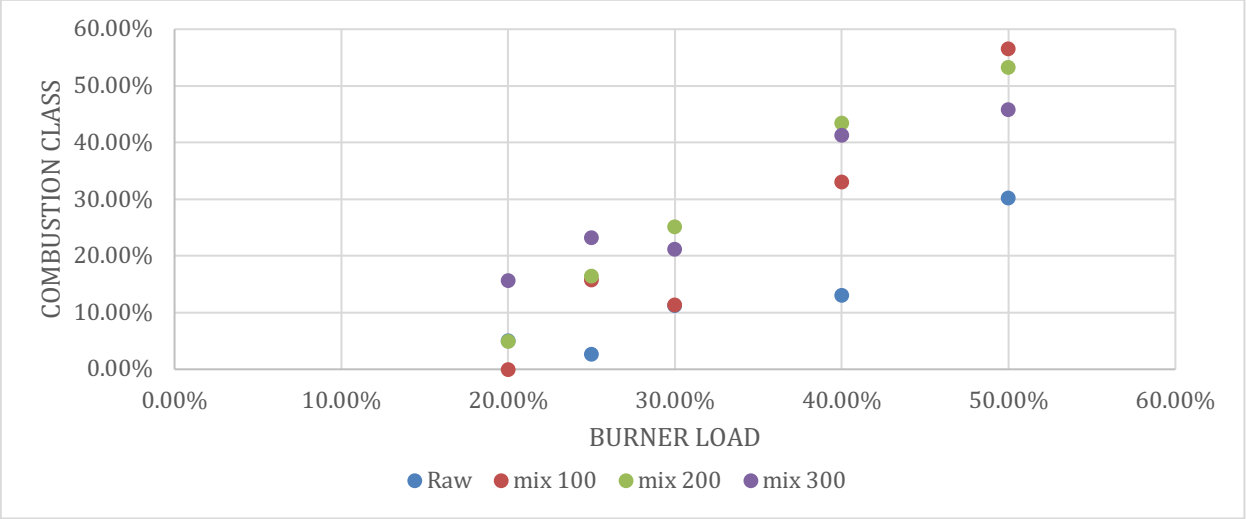

Figure 4.14 - Fuel comparison - Lambda 0.7

4.5 Techno-economic Assessment

For the Techno-economic Assessment calculations, the starting point was to define the oil consumption of a typical 800 MW boiler during a cold, warm and hot start-ups, with data provided by the client. Then to calculate the power output that each start-up provides to the boiler and convert to the equivalent amount of coal and biomass required to achieve the same power output during ignition. The relevant data is presented in Table *4.5* and Table *4.6*.

Table 4.5 - Fuels calorific values

Net Calorific Value ($MJ \cdot kg^{-1}$)	
Light oil	42.10[56]
Coal	20.37[25]
Biomass	16.32[25]

Table 4.6 - Required amount of fuel for each Ignition

Start-up	Oil consumption (ton)	Power output (MW)	Coal equivalent (ton)	Biomass equivalent (ton)
Cold	31.89	372.92	65.91	82.26
Warm	25.65	299.98	53.02	66.17
Hot	5.05	59.05	10.44	13.02

To calculate the approximate cost of each start-up, two different estimates had to be taken into consideration, first for the fuel costs, and then for the specific costs associated with the operation of each start-up. The fuel cost per metric ton, with data shared from the facility, are shown in Table 4.7. For heavy oil, a higher commercial value was used, as up to this date no data regarding the specific costs of maintenance and operation of the oil system and storage was obtained, so the costs associated with maintaining this auxiliary system was not taken into

account. For coal and biomass an assumption was made that the required milling was already comprised within the final fuel cost.

Table 4.7 - Estimated fuel costs

Fuel costs / ton	
Heavy oil	€ 933.24[57]
Coal	€ 180.00
Biomass	€ 200.00

As the plasma is only turn on during a short period of time to provide the ignition, the life expectancy of the consumable parts was much greater than normal, so a rough assumption was made to maintenance and exchange the parts is done every two years, and with that the costs were divided with the expected number of yearly start-ups. The expected number of yearly start-ups is presented in Table 4.8.

Table 4.8 - Expected start-ups per year

Cold start-up	20
Warm start-up	30
Hot start-up	10

The specific costs with the plasma operation included the energy usage of the system, and costs with the plasma consumable parts (cathode, anode, etc.), Table 4.9 shows the expected operation cost of each start-up.

Table 4.9 - Estimated operation costs for each ignition

Start-up	Oil	Coal	Biomass
Cold	€ 29 759.66	€ 12 132.78	€ 16 721.98
Warm	€ 23 939.07	€ 9 667.68	€ 13 369.29
Hot	€ 4 712.00	€ 1 933.05	€ 2 784.55

With the expected number of start-ups each year presented on Table 4.8, and the operation costs of each start-up in Table 4.9, the approximated annual operation costs were calculated, as the CO_2 emission costs for coal and oil which will reflect in the final revenue, the approximate price for each metric ton of emitted CO_2 was of € 24.86 [58], values are shown in Table 4.10. Two different revenue scenarios were taken into consideration, being the first scenario where there is no CO_2 emission costs with the ignition of any fuel, and the second scenario where the CO_2 emission cost participate in the oil and coal operation costs.

Table 4.10 - Estimated annual operation costs

Start-up cost / year	Oil	Coal	Biomass
Operation costs	€ 1 360 485.42	€ 552 316.53	€ 763 363.83
CO_2 emissions costs	€ 113 054.19	€ 151 464.34	€ -
Revenue - Scenario 1	€ -	€ 808 168.59	€ 597 121.59
Revenue - Scenario 2	€ -	€ 769 758.74	€ 710 175.78

The final investment assessment was calculated assuming the initial investment of € 3 480 000.00, being comprised of the 16 required plasma systems, one for each burner, costing € 130 000.00 each unit. The cost for retrofitting the new plasma system in all 16 burners was also accounted in the investment assessment, costing € 1 400 000.00 for the whole boiler. An interest rate of 1.89% was assumed for the whole investment. In scenario 1, the calculated return period was estimated to be 4.5 years in the case of using coal as fuel, and 6.2 years with biomass used as fuel. As in scenario 2, the values were of 4.8 and 5.2 years, for coal and biomass, respectively. Table 4.11 presents the final results with the estimated return period of the investment for scenario 1, and Table 4.12 for scenario 2.

Table 4.11 - Investment Assessment - Scenario 1

Scenario 1	Coal	Biomass
Initial Investment	€ 3 480 000.00	€ 3 480 000.00
Revenue	€ 808 168.59	€ 597 121.59
Interest rate	1.89%	1.89%
Return period (years)	4.5	6.2

Table 4.12 - Investment Assessment - Scenario 2

Scenario 2	Coal	Biomass
Initial Investment	€ 3 480 000.00	€ 3 480 000.00
Revenue	€ 769 758.74	€ 710 175.78
Interest rate	1.89%	1.89%
Return period (years)	4.8	5.2

5 Conclusions

To investigate the influence of biomass particle size on plasma-assisted ignition, several fuel samples with different particle size distribution were tested, operational parameters were varied and discussed in the results section of the study. Several conclusions can be drawn from the different behaviors each fuel presented under plasma ignition. After discussing the conclusions on each sample, suitable operating boundary conditions and empirical determination of the critical share of the fine particles to reach successful operation are proposed.

Sieved 100, sieved 200 and sieved 300 had the worst performance, neither achieved stable ignition; the amount of particles smaller than 100 μm which are believed to be responsible for the first ignition were not sufficient in any of these samples to achieve ignition. Due to the short residence time between the fuel and the plasma flame, the plasma is not able to devolatilize and ignite bigger particles. Retracting the plasma torch only proved to be an advantage at higher thermal loads, 40-50%, when the fuel has enough finer share which, overcomes the plasma-fuel imperfect interaction as the higher amount of fine particles contact the plasma flame, but this behavior was not seen with this fuels.

Raw sample proved to be a suitable fuel for thermal loads higher then 25%, as combustion class type 3 or higher was achieves in all tests; operating at excess air conditions showed to decrease the performance of the fuel, as the high velocity of air increases the heat loss and in some cases, detaches and drags the flame down in the combustion chamber.

Increasing the share of particles bellow 100 μm, showed to be an improvement, effect which is attenuated at higher thermal loads of 40%. Mix 100 is a suitable fuel for thermal loads higher than 25%, combustion class type 4 or higher was achieved in all tests in sub-stoichiometric conditions; the combustion degree increases at excess air conditions, but combustion class decreases in all thermal loads, as the raw sample.

Mix 200 follows the trend as the higher amount of fine particles improves the combustion degree, combustion class reached type 4 in all sub-stoichiometric tests for thermal load higher then 25%, as the previous fuel.

Mix 300 had the best performance of all, already expected, as it contained the higher amount of the critical share. Combustion class type 4 was reached at 20% thermal load, being this the only tested sample to produce a stable flame at this thermal load.

Table 65.1 shows the minimum conditions and the critical share of particles with size below 100 μm to reach successful ignition.

Table 5.1 - Successful ignition minimum conditions

Thermal load	20%	25%	30%
Operating lambda	0.7 – 1.1	0.6 – 0.9	0.5 – 0.9
Plasma position	"0 mm"	"0 mm"	"-40 mm"
Combustion class	4	3	4-6
Critical share	17.52 %	08.83 %	12.38 %

This research has certain limitations and allows possibilities for further research. Some parameters, as the swirl of primary and secondary air were not varied in this research. Further investigation may help better understand the interaction of the plasma flame and the fuel. Particle sizes bellow 100 μm were proven to be responsible for the first ignition, as particles between 100 μm – 200 μm will be responsible to assist, maintaining stable combustion once the plasma is turned off. The evaluation of the different parameters was performed experimentally, and the conclusions determined based on empirical and experimental results. Mathematical modeling is important to better understand the phenomena during ignition and combustion of pulverized biomass. Retrofitting the plasma system into existing power plans was shown to be economically viable as governments increase taxation on CO_2 emissions. Its relevant to notice that, as biomass particles in practice are form of non-spherical and irregular shapes, it rarely consists of particles of uniform size.

6 Assessment of the work done

6.1 Objectives Achieved

From the investigations required to define the influence of particle size on the ignition and to determine the critical share of the fine biomass particles to reach successful operation. A critical share of particles was found that allows to stable ignition at specific thermal loads is presented. Woody biomass was pulverized and samples with different particle sizes were generated. Pilot-scale experiments were performed at the 500-kW combustion facility. The empirical techno-economic study on a plasma ignition system to be retrofitted in existing power plants was also performed. Thus, all objectives were fulfilled.

6.2 Final Assessment

While investigating the possible influences of the biomass particle size on plasma-assisted ignition, several parameters and guidelines had to be taken into account; the literature on the subject is still scare, which led to many assumptions based on other criteria. The topic is of great importance as there is several power plants that currently employ an oil or gas fired start-up method.

7 References

[1] M. Scheftelowitz, R. Becker, and D. Thrän, “Improved power provision from biomass: A retrospective on the impacts of German energy policy,” *Biomass and Bioenergy*, vol. 111, pp. 1–12, Apr. 2018, doi: 10.1016/J.BIOMBIOE.2018.01.010.

[2] Bundesministerium für Wirtschaft und Technologie (BMWi), “Energiekonzept für eine umwelt schonende, zuverlässige und bezahlbare Energieversorgung,” vol. 30, no. 32, 2010.

[3] H. U. Heinrichs *et al.*, “Integrated assessment of a phase-out of coal-fired power plants in Germany,” *Energy*, vol. 126, pp. 285–305, May 2017, doi: 10.1016/J.ENERGY.2017.03.017.

[4] M. S. Roni, S. Chowdhury, S. Mamun, M. Marufuzzaman, S. Johnson, and W. Lein, “Biomass Co-Firing Technology with Policies, Challenges, and Opportunities: A Global Review Biomass Co-Firing Technology with Policies, Challenges, and Opportunities,” 2017.

[5] D. O. Glushkov *et al.*, “Experimental study of coal dust ignition characteristics at oil-free start-up of coal-fired boilers,” *Appl. Therm. Eng.*, vol. 142, pp. 371–379, Sep. 2018, doi: 10.1016/J.APPLTHERMALENG.2018.07.010.

[6] A. Demirbas, “Combustion characteristics of different biomass fuels,” *Prog. Energy Combust. Sci.*, vol. 30, no. 2, pp. 219–230, Jan. 2004, doi: 10.1016/J.PECS.2003.10.004.

[7] K. S. Kung and A. F. Ghoniem, “Multi-scale analysis of drying thermally thick biomass for bioenergy applications,” *Energy*, vol. 187, p. 115989, Nov. 2019, doi: 10.1016/J.ENERGY.2019.115989.

[8] F. Alobaid, J.-P. Busch, A. Stroh, J. Ströhle, and B. Epple, “Experimental measurements for torrefied biomass Co-combustion in a 1 MWth pulverized coal-fired furnace,” *J. Energy Inst.*, Aug. 2019, doi: 10.1016/J.JOEI.2019.07.008.

[9] M. S. R. Chowdhury, A. K. Azad, M. R. Karim, J. Naser, and A. A. Bhuiyan, “Reduction of GHG emissions by utilizing biomass co-firing in a swirl-stabilized furnace,” *Renew. Energy*, vol. 143, pp. 1201–1209, Dec. 2019, doi: 10.1016/J.RENENE.2019.05.103.

[10] “Fuels from Biomass,” 2009, pp. 43–59.

[11] J. Dai, H. Cui, and J. R. Grace, “Biomass feeding for thermochemical reactors,” *Prog. Energy Combust. Sci.*, vol. 38, no. 5, pp. 716–736, Oct. 2012, doi: 10.1016/J.PECS.2012.04.002.

[12] A. Freiberg, J. Scharfe, V. C. Murta, and A. Seidler, “The use of biomass for electricity generation: A scoping review of health effects on humans in residential and occupational settings,” *Int. J. Environ. Res. Public Health*, vol. 15, no. 2, 2018, doi: 10.3390/ijerph15020354.

[13] J. Riaza, J. Gibbins, and H. Chalmers, “Ignition and combustion of single particles of coal and biomass,” *Fuel*, vol. 202, pp. 650–655, Aug. 2017, doi: 10.1016/J.FUEL.2017.04.011.

[14] D. Chen, Y. Zheng, and X. Zhu, “Determination of effective moisture diffusivity and drying kinetics for poplar sawdust by thermogravimetric analysis under isothermal condition,” *Bioresour. Technol.*, vol. 107, pp. 451–455, Mar. 2012, doi: 10.1016/J.BIORTECH.2011.12.032.

[15] H. Fatehi, F. M. Schmidt, and X.-S. Bai, “Gas phase combustion in the vicinity of a biomass particle during devolatilization – Model development and experimental verification,” *Combust. Flame*, vol. 196, pp. 351–363, Oct. 2018, doi: 10.1016/J.COMBUSTFLAME.2018.06.025.

[16] Q. Wang, W. Zhao, H. Liu, C. Jia, and H. Xu, “Reactivity and Kinetic Analysis of Biomass during Combustion,” *Energy Procedia*, vol. 17, pp. 869–875, Jan. 2012, doi: 10.1016/J.EGYPRO.2012.02.181.

[17] M. Momeni, C. Yin, S. K. Kær, T. B. Hansen, P. A. Jensen, and P. Glarborg, “Experimental Study on Effects of Particle Shape and Operating Conditions on Combustion Characteristics of Single Biomass Particles,” *Energy & Fuels*, vol. 27, no. 1, pp. 507–514, Jan. 2013, doi: 10.1021/ef301343q.

[18] D. A. Tillman, *The combustion of solid fuels and wastes*. Academic Press, 1991.

[19] V. S. Branco Lopes, “Effect of Particle Size on the Burnout and Emissions of Particulate Matter from Biomass Combustion in a Drop Tube Furnace,” Técnico Lisboa, 2016.

[20] S. Jiménez, P. Remacha, J. C. Ballesteros, A. Giménez, and J. Ballester, “Kinetics of devolatilization and oxidation of a pulverized biomass in an entrained flow reactor under realistic combustion conditions,” *Combust. Flame*, vol. 152, no. 4, pp. 588–603, Mar. 2008, doi: 10.1016/J.COMBUSTFLAME.2007.10.001.

[21] C. Mock, H. Lee, S. Choi, and V. Manovic, “Combustion Behavior of Relatively Large Pulverized Biomass Particles at Rapid Heating Rates,” *Energy & Fuels*, vol. 30, no. 12, pp. 10809–10822, Dec. 2016, doi: 10.1021/acs.energyfuels.6b01457.

[22] H. Jiang, M. Bi, B. Li, B. Gan, and W. Gao, “Combustion behaviors and temperature characteristics in pulverized biomass dust explosions,” *Renew. Energy*, vol. 122, pp. 45–54, Jul. 2018, doi: 10.1016/J.RENENE.2018.01.063.

[23] W. Weng, M. Costa, M. Aldén, and Z. Li, “Single particle ignition and combustion of pulverized pine wood, wheat straw, rice husk and grape pomace,” *Proc. Combust. Inst.*, vol. 37, no. 3, pp. 2663–2671, Jan. 2019, doi: 10.1016/J.PROCI.2018.05.095.

[24] Y. B. Yang *et al.*, “Combustion of a Single Particle of Biomass,” *Energy & Fuels*, vol. 22, no. 1, pp. 306–316, Jan. 2008, doi: 10.1021/ef700305r.

[25] J. Ballester, J. Barroso, L. M. Cerecedo, and R. Ichaso, “Comparative study of semi-industrial-scale flames of pulverized coals and biomass,” *Combust. Flame*, vol. 141, no. 3, pp. 204–215, May 2005, doi: 10.1016/J.COMBUSTFLAME.2005.01.005.

[26] J. Li, M. C. Paul, P. L. Younger, I. Watson, M. Hossain, and S. Welch, “Prediction of high-temperature rapid combustion behaviour of woody biomass particles,” *Fuel*, vol. 165, pp. 205–214, Feb. 2016, doi: 10.1016/J.FUEL.2015.10.061.

[27] T. Gebreegziabher, A. O. Oyedun, and C. W. Hui, “Optimum biomass drying for combustion – A modeling approach,” *Energy*, vol. 53, pp. 67–73, May 2013, doi: 10.1016/J.ENERGY.2013.03.004.

[28] J. Li, M. C. Paul, and K. M. Czajka, “Studies of Ignition Behavior of Biomass Particles in a Down-Fire Reactor for Improving Co-firing Performance,” *Energy & Fuels*, vol. 30, no. 7, pp. 5870–5877, Jul. 2016, doi: 10.1021/acs.energyfuels.6b01065.

[29] G. Xu, M. Li, and P. Lu, “Experimental investigation on flow properties of different biomass and torrefied biomass powders,” *Biomass and Bioenergy*, vol. 122, pp. 63–75, Mar. 2019, doi: 10.1016/J.BIOMBIOE.2019.01.016.

[30] J. Li, A. Brzdekiewicz, W. Yang, and W. Blasiak, “Co-firing based on biomass torrefaction in a pulverized coal boiler with aim of 100% fuel switching,” *Appl. Energy*, vol. 99, pp. 344–354, Nov. 2012, doi: 10.1016/J.APENERGY.2012.05.046.

[31] H. Rezaei, S. Sokhansanj, X. Bi, C. J. Lim, and A. Lau, “A numerical and experimental study on fast pyrolysis of single woody biomass particles,” *Appl. Energy*, vol. 198, 2017, doi: 10.1016/j.apenergy.2016.11.032.

[32] H. Fatehi *et al.*, “Numerical simulation of ignition mode and ignition delay time of pulverized biomass particles,” *Combust. Flame*, vol. 206, pp. 400–410, Aug. 2019, doi: 10.1016/J.COMBUSTFLAME.2019.05.020.

[33] V. Branco and M. Costa, “Effect of particle size on the burnout and emissions of particulate matter from the combustion of pulverized agricultural residues in a drop tube furnace,” *Energy Convers. Manag.*, vol. 149, pp. 774–780, Oct. 2017, doi: 10.1016/J.ENCONMAN.2017.03.012.

[34] J. Steer, “The effects of particle grinding on the burnout and surface chemistry of coals

in a drop tube furnace," *Fuel*, vol. 160, pp. 413–423, 2015, doi: 10.1016/j.fuel.2015.07.094.

[35] H. Lu, E. Ip, J. Scott, P. Foster, M. Vickers, and L. L. Baxter, "Effects of particle shape and size on devolatilization of biomass particle," *Fuel*, vol. 89, no. 5, pp. 1156–1168, May 2010, doi: 10.1016/J.FUEL.2008.10.023.

[36] C. Yin, S. K. Kær, L. Rosendahl, and S. L. Hvid, "Co-firing straw with coal in a swirl-stabilized dual-feed burner: Modelling and experimental validation," *Bioresour. Technol.*, vol. 101, no. 11, pp. 4169–4178, Jun. 2010, doi: 10.1016/J.BIORTECH.2010.01.018.

[37] J. Saastamoinen, M. Aho, A. Moilanen, L. H. Sørensen, S. Clausen, and M. Berg, "Burnout of pulverized biomass particles in large scale boiler – Single particle model approach," *Biomass and Bioenergy*, vol. 34, no. 5, pp. 728–736, May 2010, doi: 10.1016/J.BIOMBIOE.2010.01.015.

[38] J. M. Jones, L. I. Darvell, T. G. Bridgeman, M. Pourkashanian, and A. Williams, "An investigation of the thermal and catalytic behaviour of potassium in biomass combustion," *Proc. Combust. Inst.*, vol. 31, no. 2, pp. 1955–1963, Jan. 2007, doi: 10.1016/J.PROCI.2006.07.093.

[39] A. Di Gianfrancesco, "The fossil fuel power plants technology," *Mater. Ultra-Supercritical Adv. Ultra-Supercritical Power Plants*, pp. 1–49, Jan. 2017, doi: 10.1016/B978-0-08-100552-1.00001-4.

[40] D. I. Barnes, "Understanding pulverised coal, biomass and waste combustion – A brief overview," *Appl. Therm. Eng.*, vol. 74, pp. 89–95, Jan. 2015, doi: 10.1016/J.APPLTHERMALENG.2014.01.057.

[41] P. Holmgren *et al.*, "Size, shape, and density changes of biomass particles during rapid devolatilization," *Fuel*, vol. 206, pp. 342–351, Oct. 2017, doi: 10.1016/J.FUEL.2017.06.009.

[42] S. Li, S. Xu, S. Liu, C. Yang, and Q. Lu, "Fast pyrolysis of biomass in free-fall reactor for hydrogen-rich gas," *Fuel Process. Technol.*, vol. 85, no. 8–10, pp. 1201–1211, 2004, doi: 10.1016/j.fuproc.2003.11.043.

[43] B. Göktepe, A. H. Saber, R. Gebart, and T. S. Lundström, "Cold flow experiments in an entrained flow gasification reactor with a swirl-stabilized pulverized biofuel burner," *Int. J. Multiph. Flow*, vol. 85, pp. 267–277, Oct. 2016, doi: 10.1016/J.IJMULTIPHASEFLOW.2016.06.016.

[44] M. Sugimoto, K. Maruta, K. Takeda, O. P. Solonenko, M. Sakashita, and M. Nakamura,

"Stabilization of pulverized coal combustion by plasma assist," *Thin Solid Films*, vol. 407, no. 1–2, pp. 186–191, Mar. 2002, doi: 10.1016/S0040-6090(02)00035-4.

[45] W. Li, K. Cen, C. Zheng, J. Zhou, and X. Cao, "Induction-heating ignition of pulverized coal stream," *Fuel*, vol. 83, no. 16, pp. 2103–2107, Nov. 2004, doi: 10.1016/J.FUEL.2004.06.011.

[46] S. Belosevic, M. Sijercic, and P. Stefanovic, "A numerical study of pulverized coal ignition by means of plasma torches in air–coal dust mixture ducts of utility boiler furnaces," *Int. J. Heat Mass Transf.*, vol. 51, no. 7–8, pp. 1970–1978, Apr. 2008, doi: 10.1016/J.IJHEATMASSTRANSFER.2007.06.003.

[47] K. Zhang, L. Liu, H. C. Schröder, and G. Feng, "Plasma Ignition System for the Oil-free Power Plant Zetes in Turkey and its Advantages for the Changed Circumstance of the Energy Market," in *Kraftwerks Kolloquim*, 2017, pp. 293–303.

[48] V. E. Messerle, A. B. Ustimenko, A. S. Askarova, and A. O. Nagibin, "Pulverized coal torch combustion in a furnace with plasma-coal system," *Thermophys. Aeromechanics*, vol. 17, no. 3, pp. 435–444, Sep. 2010, doi: 10.1134/S0869864310030145.

[49] V. E. Messerle, A. B. Ustimenko, Y. E. Karpenko, M. Y. Chernetskiy, A. A. Dekterev, and S. A. Filimonov, "Modeling and full-scale tests of vortex plasma-fuel systems for igniting high-ash power plant coal," *Therm. Eng.*, vol. 62, no. 6, pp. 442–451, Jun. 2015, doi: 10.1134/S0040601515060063.

[50] E. I. Karpenko, V. E. Messerle, and A. B. Ustimenko, "Plasma-aided solid fuel combustion," *Proc. Combust. Inst.*, vol. 31 II, no. 2, pp. 3353–3360, 2007, doi: 10.1016/j.proci.2006.07.038.

[51] V. E. Messerle, E. I. Karpenko, and A. B. Ustimenko, "Plasma assisted power coal combustion in the furnace of utility boiler: Numerical modeling and full-scale test," *Fuel*, vol. 126, pp. 294–300, Jun. 2014, doi: 10.1016/J.FUEL.2014.02.047.

[52] "Description of the 0.5 MW Pilot Testing Facility at IFK."

[53] R. Youssefi, J. Maier, and G. Scheffknecht, "Experimental Investigations on Biomass Ignition with the Support of a Plasma Torch," 2019, no. September.

[54] M. Hammad Baig, "Determination of ignition and combustion boundaries in a pilot pulverized fuel burner," University of Stuttgart, 2018.

[55] ASTM B214-07, "Standard Test Method for Sieve Analysis of Metal Powders," *Annu. B. ASTM Stand.*, pp. 7–10, 2007.

[56] A. Saario, A. Rebola, P. J. Coelho, M. Costa, and A. Oksanen, "Heavy fuel oil combustion

in a cylindrical laboratory furnace: measurements and modeling," *Fuel*, vol. 84, no. 4, pp. 359–369, Mar. 2005, doi: 10.1016/J.FUEL.2004.10.002.

[57] "Germany heating oil prices, 25-Nov-2019." [Online]. Available: https://www.globalpetrolprices.com/Germany/heating_oil_prices/. [Accessed: 28-Nov-2019].

[58] "CO2 European Emission Allowances PRICE | Markets Insider." [Online]. Available: https://markets.businessinsider.com/commodities/co2-european-emission-allowances. [Accessed: 28-Nov-2019].

Appendix A – PSDs

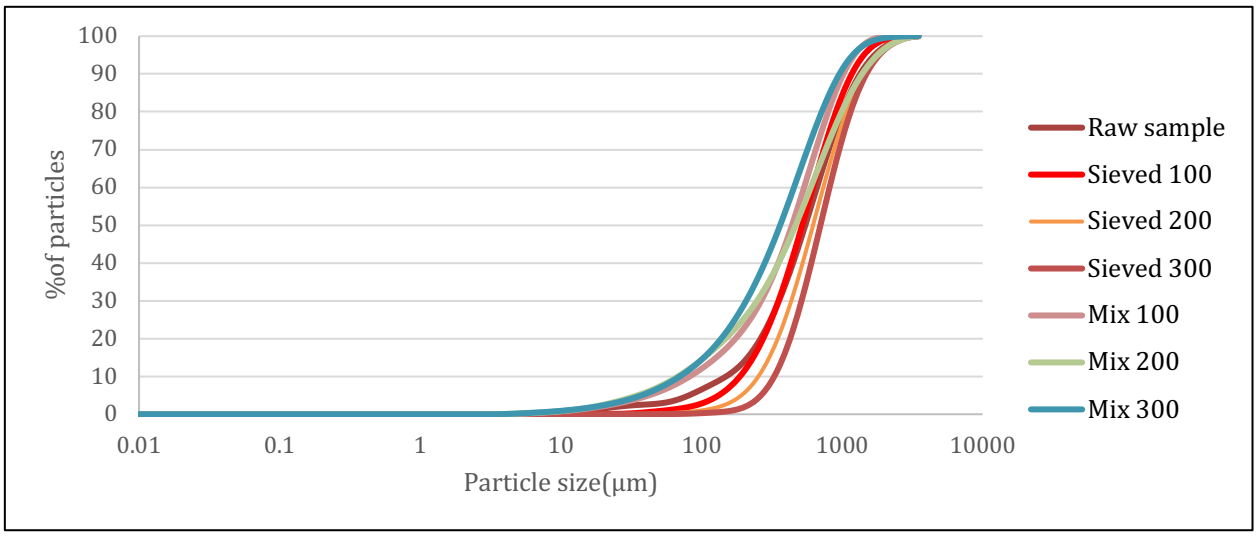

Figure A.1 - Cumulative size Distribution - Volumetric

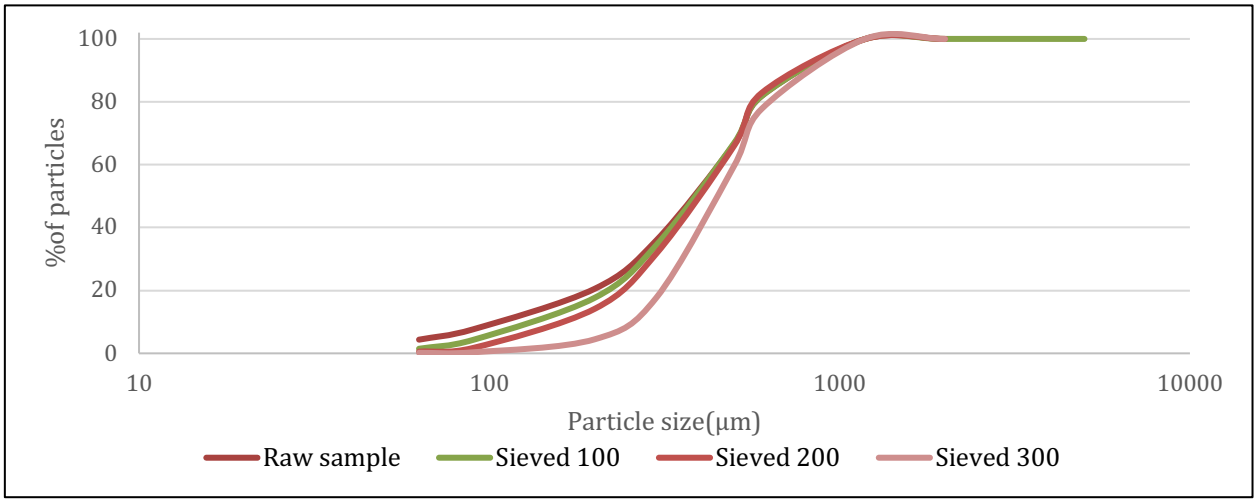

Figure A.2 - Cumulative size Distribution - Mass

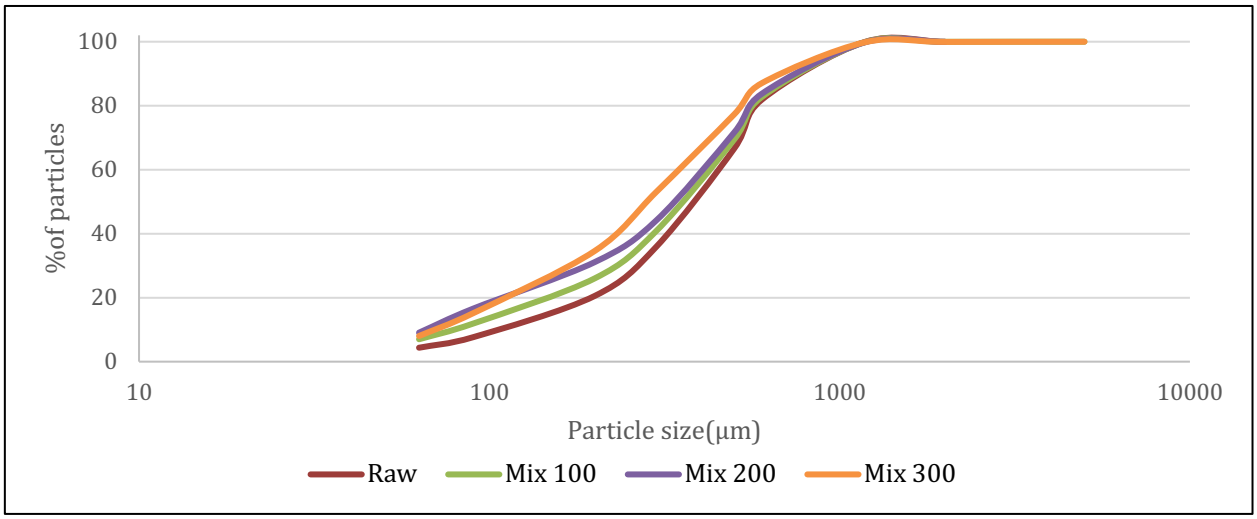

Figure A.3 - Cumulative size Distribution - Mass

Appendix B – Test Matrix

Figure B.1 shows an example of the test matrix used to assist during the tests.

WP- 3 kW-PIAP													
Themal power (kW)	% of full load	biomass (kg/h)	Dosier (mA)	Primary air (Nm3/h)	fuel/air (kg/kg)	plasma power (kW)	lambda	Second air (Nm3/h)	total air	position "0 mm" time	position "0 mm" remark	position "-40" time	position "-40" remark
100	33.33	20.7	4.6	30	0.53	3.00	0.6	25.0	55				
							0.7	35.0	65				
							0.9	54.0	84				
125	41.67	25.9	5.7	30	0.67	3.00	0.6	39.0	69				
							0.7	51.0	81				
							0.9	74.4	104				
							1.1	97.6	128				
150	50	31.06	6.8	30	0.80	3.00	0.5	40.0	70				
							0.6	53.0	83				
							0.7	68.0	98				
							0.9	96.0	126				
							1	110.0	140				
							1.1	124.0	154				
200	66.67	41.41	9.1	30	1.07	3.00	0.5	63.0	93				
							0.6	81.4	111				
							0.7	100.0	130				
							0.9	137.0	167				
							1.1	174.0	204				
250	83.33	51.76	11.4	30	1.33	3.00	0.5	86.0	116				
							0.7	132.0	162				
							0.9	179.0	209				
							1.1	225.0	255				
300	100.00	62.11	13.7	30	1.60	3.00	0.7	165.0	195				
							0.9	221.0	251				
							1.1	276.0	306				

Figure B.1 - Test matrix